UNIVERSITY OF TROMSØ UIT

FACULTY OF SCIENCE AND TECHNOLOGY
DEPARTMENT OF PHYSICS AND TECHNOLOGY

Suppression of fingering instabilities in superconductors by magnetic braking

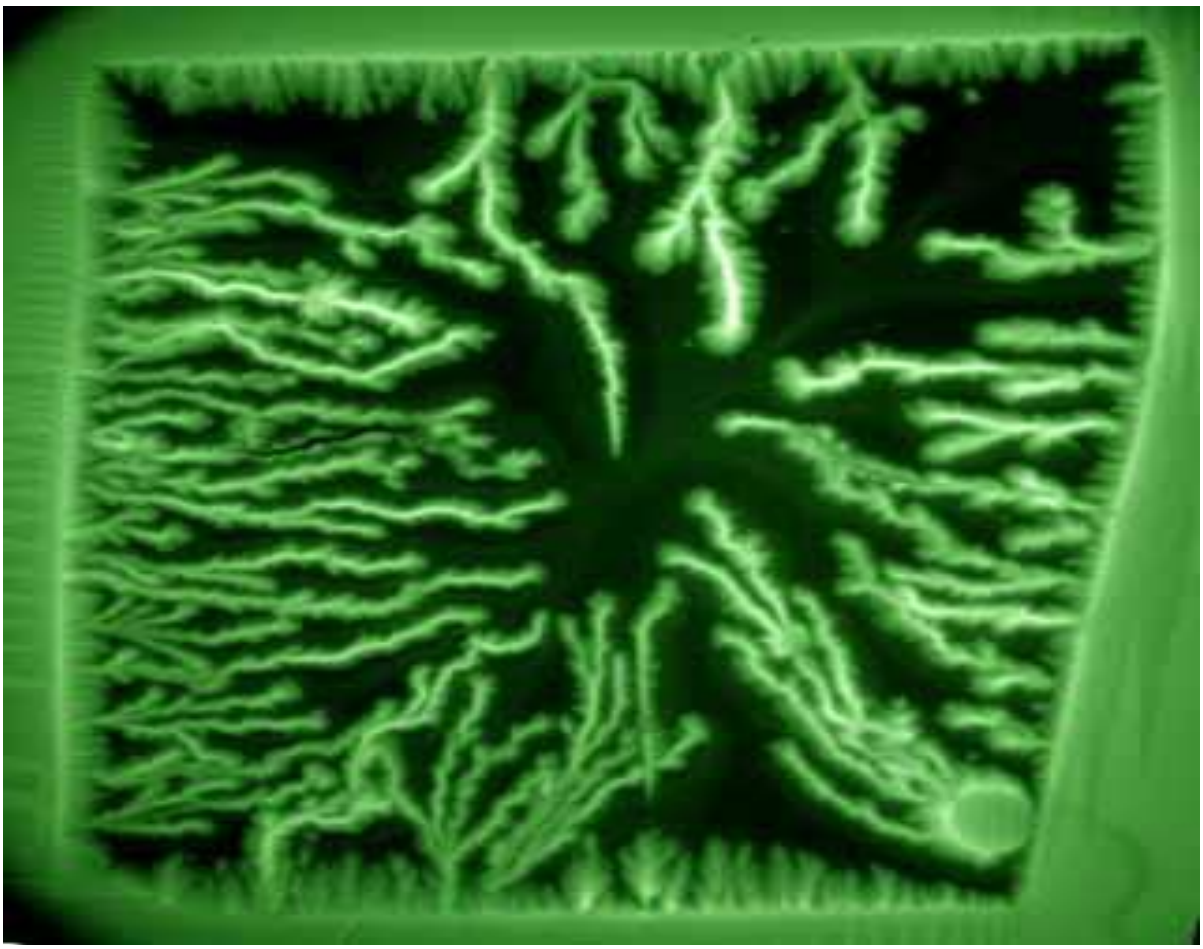

Original by: SC group at UIO

Elijah Lator

FYS-3900 Master's Thesis in Physics

November 2012

Acknowledgements

After one year of adventures on superconductivity, this thesis is ready. It is with pleasures and sincere thanks that I acknowledge the help, support and encouragement I have received while working on this thesis. My first contact with superconductivity research was during our class visit in the laboratory of condensed physics at University of Oslo. I was fascinated to see the image of magnetic avalanches in superconductor with MOI (magneto-optical imaging). I took contact with my former teacher of nanophysics Yuri Galperin about writing a thesis in magnetism and superconductivity. He pointed me to Jorn Inge Vestgaarden and Danill Shantsev.

I feel very privileged as I have been conducting my Master research under their supervisions by knowing that the superconductivity group in Oslo is one of the best in this field. First of all, I would like to express my deeply-felt thanks to Jorn Inge Vestgaard for his warm encouragement and thoughtful guidance. Discussions with him allowed me to understand more about superconductivity and the best way to start my thesis.

I thank my other cosupervisor Danill Shantsev. Despite his busy schedule, he always came to help me to find simple solution to one complicated problem. It was interesting to discuss with Pavlo Mikheenko about MOI and I am interested to gain much knowledge about this microscope in the future. I thank my classmate Atta Monem Ayaz for his help how to use latex on windows.

For peoples in Tromso, I would like to thank student adviser Geir Antonsen, professor Kenneth Ruud and professor Ruth Esser. I thank Geir Antonsen for having make it possible to present my Master thesis at University of Tromso. I thank professor Kenneth Ruud for being my main supervisor and I strongly valued your many comments and constructive criticism on my manuscript. Thanks to professor Ruth Esser for having give me hope to learn more about physics.

Finally, I would like to thank my family for his support and love. Special thanks to my brother Cedric W. Kasongo, who always makes me laugh with his jokes about physics. For example, he told me once the story of Newton's laws:

A Cow was walking. NEWTON stopped it. It stopped.
He found his first law,
"An object continues to move unless it's
stopped".

He gave a FORCE by kicking the Cow, it gave a Sound "MA"!
He formulated the 2nd law, F=MA!!

After sometime the Cow gave a kick to Newton,

then he formulated the 3rd Law.
i.e, 'EVERY ACTION HAS AN EQUAL AND OPPOSITE.

.

Innhold

.

Chapter 1

1 Introduction

1.1 Short word about the history of Superconductor

Superconductivity was discovered in 1911 by Heike Kamerlingh Onnes and it fast became one of the most important phenomena in modern physics. When Onnes cooled mercury to the temperature of liquid helium, 4 degrees Kelvin (-452F, -269C), its resistance suddenly disappeared. It was necessary for Onnes to come within 4 degrees of the coldest temperature that is theoretically attainable to witness the phenomenon of superconductivity. Later, in 1913, he won a Nobel Prize in physics for his research in this area. Superconductors are materials that can transport electrical current without resistance and loss of energy.

In addition to being able to conduct electrical current without resistance, superconductors also have an extraordinary magnetic property. As a general rule, superconductor will repel the magnetic field. However, in many cases the magnetic field can nevertheless penetrate the superconductor only in the form of minute quantized lines [35]. These lines easily become pinned inside the material.

All these facts make superconductor very promising materials for application in science, in industry, in medicine, etc. However, there is a serious lack to these materials- the superconductors exist only at very low temperature. The first discovered superconducting materials had the transition temperature not higher than 20 K and BCS theory forbade the existence of superconductor with critical temperature of more than 30 K. But in 1986, high temperature superconductor(HTCS which has a critical temperature more than what BSC predicted)$LaBaCuO$ was discovered by Bednorz and Muller [12].

This discovery was followed by a long range of new superconducting materials with high critical temperature. Even if the structure of HTCS is not easy to produce, it made them not well suited for industry; they are brittle(hard to make cable) and have poor critical density j_c at 77 K.In my thesis i work with the superconductor called magnesium diboride MgB_2(with critical temperature $T_c \approx 39K$. It has unique properties and it is very easy to produce and to use in commercial applications [9].

1.2 Motivation for this thesis

This thesis is a theoretical investigation problem about the thermomagnetic instability in superconductor and its suppression by deposing a metallic layer. It is known from the first papers on thermomagnetic instability that the flux jumps in superconducting sample could be cured by the superconductors being thermally stabilized after having been coated with metal[2],[3] and [48]. It was strongly suggested that the thermal conductor/contact greatly suppresses the vortex avalanches.

Recently, experiments [5] and [49] showed that one observes the suppression of avalanches even if the deposited metal is not in contact with superconductor. This means that the origin of stability in superconductor coated with metal is not fully due to thermal contact. Several experiment papers [5], [7] suggested that the phenomenon is electrodynamic braking origin. My work is focused on this effect. The meaning is to apply the old theory about the thermo-magnetic instability to a new model for electrodynamic braking for investigating the suppression of avalanches with metal. In others words, it is already known from experiment that it works, but the goal of thesis is to prove that it works theoretically.

Phenomena has recently attracted much attention, not only for his importance in commercial applications, in many scientific fields. For example, it was suggested that the thermomagnetic instability in superconducting cable could be responsible for the magnet quench incident at LHC(Large Hadron Collider). CERN released a preliminary analysis of the incident on October 2008 and a more detailed one on 5 December 2008. Both analyses confirmed that the incident was indeed initiated by a faulty electrical connection [35]. My thesis can be usefully in such analysis since it is a study of thermomagnetic instability in superconducting bulk than in thin films.

1.3 General description of thermomagnetic instability

An applied magnetic field penetrates a superconductor in the mixed-state (also known as the vortex state), where the vortices are quantized. This quantized flux is called Abrikosov vortices. The supercurrent circulates around the normal(i.e. non-superconducting) core of the vortex. As the applied field increases, the density of vortices also increases and the cores begin to overlap, which in turn make the vortex-vortex nearest-neighbor distance smaller than the penetration depth. At high density the internal field becomes very large and the variation of the field in the space between the cores becomes very small. When the penetration depth is much larger than the coherence length (see definition in subsection 1.5.2, Eq.10), as is usually the case with the high-temperature superconductors, there is considerable overlap of vortices throughout most of the mixed-state range, and the magnetic flux is present mainly in the surrounding region, rather than in the actual cores. The presence of the applied field at the surface of the superconductor induces vortices to form right inside the surface. An increase in the applied field causes more vortices to enter and move inward by diffusion and by virtue of mutual repulsion due to thermomagnetic instability. Some vortices become pinned during migration.

Concerning the flux motion that takes place at superconductor type-II (which contains vortices state), there are two kind of them, called "flux creep " and " flux flow". For low currents the vortices hop from one pinning center to another and this motion is thermally activated,this is the flow creep. If the pinning instead is weak in comparison to the Lorentz force, vortices move with a steady viscous motion, in which the driving force is balanced by a friction force. This regime is called flux flow. For weak pinning the vortex lattice reacts elastically to an applied force, such as Lorentz force from a transport current. For strong pinning, non-trapped vortices move past trapped vortices and flux flows along channels between regions of trapped flux. This later involves groups of vortices moving cooperatively as a unit, and form flux bundles. Energy barriers can hinder flux creep which involves thermally activated jumps of flux bundles. The flux jump that we observe in superconductors is the instability that drives the system from flux creep to flux flow. This flux jumping is commonly observed at low temperatures in type-II superconductors with strong pinning.

It is difficult to be able to see how magnetic lines penetrate bulk superconducting sample and

become pinned inside. But the superconductivity research group in Oslo developed a magneto-optical imaging technique with which it is possible to directly see these lines as they penetrate thin films and become pinned inside. Here are these flux patterns in dendritic structure due to thermomagnetic instability. As consequence, the pinning force will be reduced and make it easier for more vortices to move into the sample and these flux avalanches is visualized with magneto-optical imaging (see Fig 1).

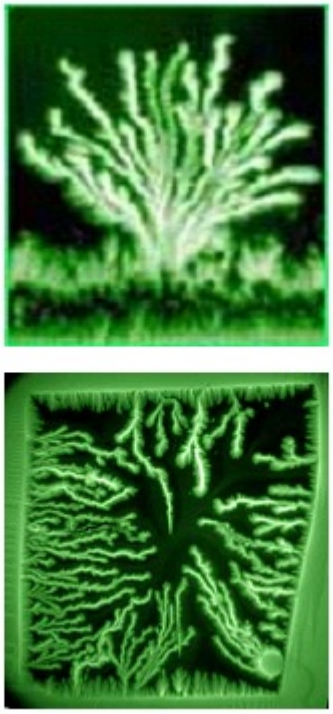

Figur 1: *Dendritic flux structures seen on the image where they abruptly penetrate the film in response to slowly increasing applied field. Bright green color corresponds to magnetic field penetrated into body of superconductor. The dendrites were formed at applied field 17 mT and temperature 9.9 K. Pictures are taken from the internet site of Superconductivity Laboratory at the University Oslo (http://WWW.fys.uio.no/super/)*

If we manage to control the way in which dendritic patterns are distributed and pinned inside the superconductor, this will be the key to improve the electromagnetic properties of the material. For example, we shall be able to locate directly the weak and good parts, the pinning and non-pinning parts of the superconductor. This instability can be the reason for magnetic noises; they reduce the effective critical current density and they can even lead to total malfunction of superconducting device [34]. One possibility to reduce and suppress this instability is to coat the superconducting sample with a metallic layer. The MOI (magneto-optical imaging)clearly showed that the deposition of metallic gold on top of improved its thermal stability and suppressed the sudden appearance of dendritic flux avalanches [see Fig 2].

There are two fundamental supports that explain the reason for thermomagnetic instability in superconductors:

(i) The motion of magnetic flux releases energy, thereby increasing the local temperature;

(ii) The temperature rising decreases flux pinning, thereby facilitating the flux motion.

Based on the qualitative explanation given above, , we can see that there are several parameters which play an important role in thermomagnetic instability, including critical current density, thermal conductivity, electric conductivity, heat capacity, and critical temperature. Let take briefly a closer look at these thermal properties because they are useful for the later analysis.

1.4 Materials parameters

The application of a sufficiently strong magnetic field to a superconductor causes its resistance to return to the normal state value, and when the total current density reaches a certain value, normally the critical current density , the superconductor starts returning to ohmic state and its resistivity increases drastically. The critical current density is temperature dependent $j_c = j_{c0}(1-\frac{T}{T_c})$.

The specific heat has traditionally been regarded as a physical property of superconductor that scales with the size of physical system in the development of theory of superconductivity. The phonon contribution to specific heat capacity is important when the temperature T is away from critical temperature T_c. In the present study, we are looking at the penetration of B-field in superconducting sample. Assuming the thermomagnetic instability that takes place in the process,the phonon contribution can be neglected since the process is under T_c. Also, in this thesis the heat capacity is $C_s \simeq \ C_s(T_c)(\frac{T}{T_c})^3$.

We know from thermodynamics that the thermal conduction involves the transport of entropy. For superconductivity state, the entropy goes continuously to zero. The explanation for this is that the superconducting electrons don't carry entropy. The onset of superconductivity can have the effect of first increases the conductivity until it reaches a maximum, beyond which it decreases lower temperature. Also, the thermal conductivity is consequence of the energy gap led from electron-lattice-electron interaction(see more about BCS mechanism in [38]).Thermal conductivity is proportional to heat capacity and in this thesis is $\kappa \simeq \kappa(T_c)(\frac{T}{T_c})^3$.

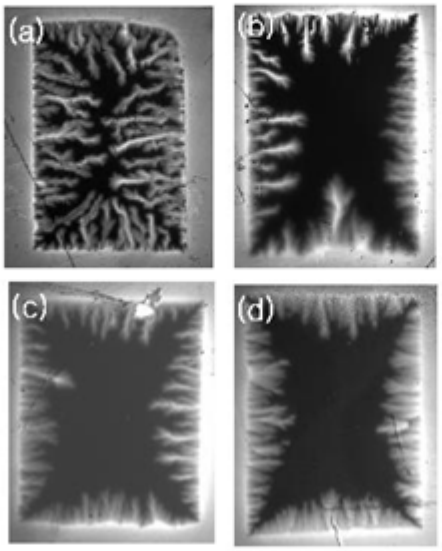

Figur 2: *Magneto optical (MO) images of flux penetrations into the virgin states of MgB_2 thin films at 3.8 K for gold thickness of (a) 0, (b) 0.2, (c) 0.9, and (d) 2.55*Âμm*. The images were taken at an applied field of 34mT. Pictures are taken from the internet site Eun-,I CChoi.*

1.5 Ginzburg- Landau Theory

1.5.1 Ginzburg-Landau equation

Ginzburg-Landau theory is a mathematical theory used to describe superconductivity. Initially, it was proposed by Landau as a phenomenological model which could describe type-I superconductor without examining their microscopic properties. Ginzburg was very impressed by this Landau's work on phase transitions and had been thinking about how to apply it to the phase transitions inside superconductors.

Based on Landau's established theory of second-order phase transitions, both Landau and Ginzburg suggested that the free energy , for a superconductor near the superconducting transition can be expressed in terms of a complex order parameter field Ψ , which magnitude describes how deep in superconducting phase the system is. For a complex order parameter the Landau expansion of the free energy for small$|\Psi|$ would be

$$F = \int [\alpha(T)|\Psi|^2 + \frac{1}{2}\beta|\Psi|^4 + \gamma(T)|\bigtriangledown\Psi|^2]d^3x \tag{1}$$

For a charged superfluid we must add the coupling to the vector potential and also the magnetic energy, so that the full expression for a pair-superconductor can be written as:

$$F = \int [\alpha(T)|\Psi|^2 + \frac{1}{2}\beta|\Psi|^4 + \gamma(T)|(\nabla + \frac{2ie}{\hbar c}\vec{A})\Psi|^2 + \frac{B^2}{8\pi\mu_0}]d^3x \tag{2}$$

Near the transition temperature, we can write $\alpha(\top) \approx \alpha(\top - \top_c), \beta(\top) \approx \beta.$,and take $\alpha, \beta and \gamma$ to be independent of temperature $\top$.The free energy F must be minimized with respect to variation of Ψ and $\vec{A}$:

$$\frac{\delta F}{\delta A} = 0 = -\frac{2e\gamma}{\hbar c} i[\Psi^*(\nabla + \frac{2ie}{\hbar c}\vec{A})\Psi - \Psi(\nabla - \frac{2ie}{\hbar c}\vec{A})\Psi^*] + \frac{1}{4\pi}\nabla \times (\bigtriangledown \times \vec{A}) \tag{3}$$

or $\bigtriangledown \times \tilde{B} = (\frac{4\pi}{c}\vec{j})$, with $j = -\frac{4e}{\hbar}\gamma|\Psi|^2(\nabla\phi - \frac{2e}{\hbar c}\vec{A})$.

Minimizing with respect to it gives Ginzburg-Landau equation ,

$$\alpha|\Psi|^2 + \frac{\beta}{2}|\Psi|^2\Psi + \frac{1}{2m}(-i\hbar\nabla - 2e\vec{A})^2\Psi = 0 \tag{4}$$

$$\vec{j} = \frac{2e}{m} Re\Psi^*(-i\hbar\nabla - 2e\vec{A})\Psi \tag{5}$$

where $\vec{j}$ denotes the dissipation-less electrical current density.

The first equation determines the order parameter Ψ, based on the applied magnetic field. The second equation then provides the superconducting current. Assuming the smallness of$|\Psi|$ and the smallness of its gradients, the free energy has the form of a field theory such that in (2)and(3) can be written in the simple concise form:

$$F = F_n + \alpha|\Psi|^2 + \frac{\beta}{2}|\Psi|^4 + \frac{1}{2m}|(-i\hbar\nabla - 2e\vec{A})\Psi|^2 + \frac{\vec{\beta^2}}{2\mu_0} \tag{6}$$

where F_n is the free energy in the normal phase,α and β in the initial argument were treated as phenomenological parameters,m is the effective mass,e is the elementary charge($\pm 2e$), $\vec{A}$is the magnetic vector potential, and $\vec{B} = \vec{\bigtriangledown} \times \vec{A}$ is the magnetic field. The physical interpretation here

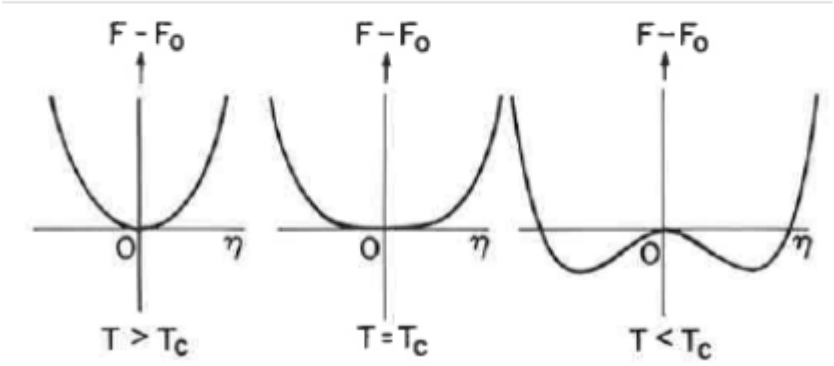

Figur 3: *difference between Helmholtz free energy density in the superconducting($\alpha < 0$ or $T < T_c$) and normal ($\alpha > 0$ or $T > T_c$) state, depending on the order parameter in the Ginzburg-Landau theory.*

is explained in a simple way, see in article [18]. Consider a homogeneous superconductor where there is no superconducting current. The equation forΨ simplifies to:

$$\alpha|\Psi|^2 + \frac{\beta}{2}|\Psi|^2\Psi = 0 \tag{7}$$

This equation has a trivial solution:$\Psi = 0$. This corresponds to the normal state of the superconductor, that is for temperature$T$ beyond the superconducting transition temperature,T_c. Below the superconducting transition temperature, the above equation is expected to have a non-trivial solution (when$\Psi \neq 0$). Under this assumption the equation above can be rearranged into:

$$|\Psi|^2 = -\frac{\alpha}{\beta} \tag{8}$$

Bear in mind that the magnitude of a complex number can be either positive or zero. This means that there is non-zero solution forΨ when the right-hand side of the equation (7)is positive.

This can be achieved by assuming the following temperature dependence of α, $\alpha(T) = \alpha_0(T - T_c)$ with $\frac{\alpha_0}{\beta}$:

* Above the superconducting transition temperature, $T > T_c$, the expression $\frac{\alpha(T)}{\beta}$ is positive and the right-hand side of the equation (7) is negative. We early said that the magnitude of a complex number must be a non-negative number, so onlyΨ solves the Ginzburg-Landau equation.

* Below the superconducting transition temperature, , the right-hand side of the equation(7) is positive and there is a non-trivial solution for Ψ. When approaches zero as gets closer to from below, we get

$$|\Psi|^2 = -\frac{\alpha_0(T - T_c)}{\beta} \tag{9}$$

1.5.2 Coherence length and London penetration depth

Ginzburg-Landau equations predicted the existence of two characteristic lengths in a superconductor. These are the London penetration depth and the coherence length. The London penetration depth λ_L is a fundamental length that characterizes a superconductor and is given by

$$\lambda = \sqrt{\frac{m}{4\mu_0 e^2 \Psi_0^2}} \tag{10}$$

Where Ψ_0 is the equilibrium value of the order parameter in the absence of an electromagnetic field.

The penetration depth sets the exponential law according to which an external magnetic field decays inside the superconductor. Ginzburg-Landau therory predicted this new length ξ.The coherence length is a measure of the distance within which the superconducting electron concentration cannot change drastically in a spatially-varying magnetic field. The coherence length, ξ , is given by

$$\xi = \sqrt{\frac{\hbar^2}{2m|\alpha|}} \tag{11}$$

It sets the exponential law according to which small perturbations of density for superconducting electrons recover their equilibrium value Ψ_0.

The ratio $\kappa = \frac{\lambda_L}{\xi}$ is known as the Ginzburg-Landau parameter. Although λ_L and ξ depend strongly on temperature,but they mainly cancel out in the ratio, and κ is roughly temperature independent. This parameter κ determines the nature of the behaviour in a magnetic field since λ and ξ come from quite different physics,κ varies from small to large values in different materials. It has been shown that the domain-wall surface energy of the superconductor was positive for $\kappa < \frac{1}{\sqrt{2}}$ and negative for $\kappa > \frac{1}{\sqrt{2}}$.

1.5.3 Superconductor type I and type II

There is not just one criterion to classify superconductors, but they are divided into two most common types:

1. Type I: if Ginzburg-Landau parameter $\kappa < \frac{1}{\sqrt{2}}$,it means they have a single critical field, above which all superconductivities are lost. Type I completely satisfies the Meissner effect, which can be defined as the spontaneous expulsion of the internal magnetic field during transition into superconductivity.

2. Type II: If Ginzburg-Landau parameter $\kappa > \frac{1}{\sqrt{2}}$, it means they have two critical fields, between which they partial allow penetration of the magnetic field. Type II does not completely satisfy Meissner effect and the vortex state is found between these two critical fields.

The result of the thesis considered type II superconducting specimen since thermo-magnetic instability can only take place in mixed state or vortex state that occurs in type-II superconductors.

1.6 Superconductor MgB_2

The formalism of the thesis is general for type-II superconductors, but the numerical values are from magnesium diboride MgB_2. The magnesium diboride is a simple ionic binary compound that has proven to be an inexpensive and useful superconducting material. It was discovered by Nagamatsu and coworkers [53]. Its structure is shown in figure 4 and can be viewed as a simple hexagonal stacking of graphitic boron with a magnesium atom above and below the center of each boron hexagon.

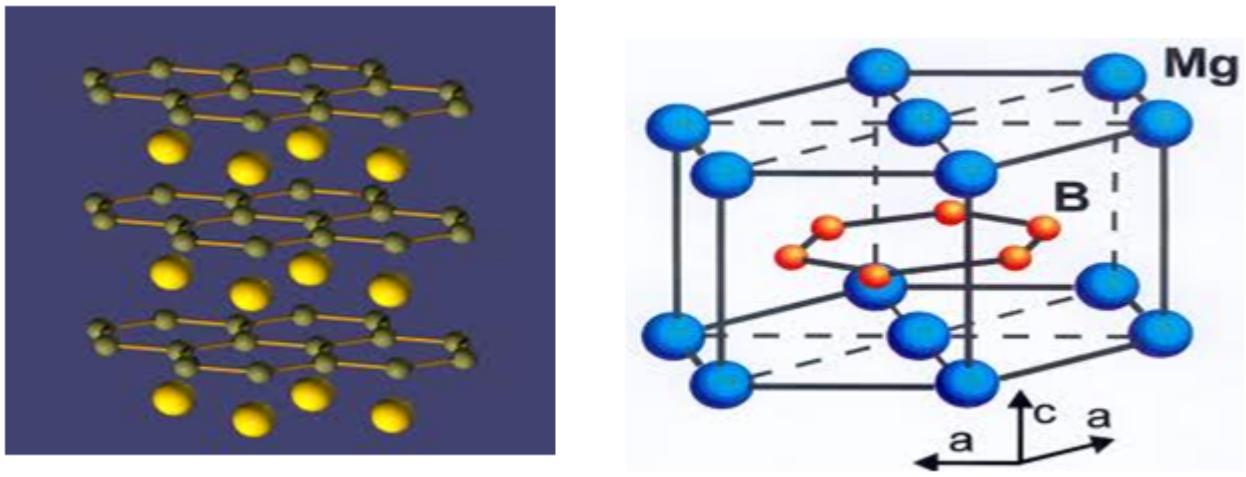

Figur 4: *The structure of magnesium diboride, Magnesium in blue color and Boron in yellow/red color (image from [45] grants anyone the right to use this work for any purpose, without any conditions, unless such conditions are required by law).*

Its critical temperature is 39 K and the honeycomb planes of Boron atoms remains the structure of graphite, which plays the most important role in electronic properties. The conventional theory says that Magnesium diboride is type-II. But there has been proposed that it is both type I and type II [47]. Recently a theory called "1.5 Type Superconductivity" has been proposed [54]. The argument is that this theory is characterized by two coherence lengths such that their inter-vortex interaction is attractive at long range and repulsive at short range. One observes these properties in MgB_2. This should give vortex long-range attractive, short-range repulsive interaction. Yet, critics of the proposed theory say that the two bands interact and if one includes this interaction you will end up with just one order parameter, as in classical G-L theory[55].

MgB_2 has two energy gaps, and for one band $\kappa < \frac{1}{\sqrt{2}}$ and for the other $\kappa > \frac{1}{\sqrt{2}}$. Like for graphite, MgB_2 has strong σ bonds in the planes and weak π-bonds between planes. Unlike for graphite, B atoms in MgB_2 has fewer electrons than carbon atoms. Not all the bonds for Boron planes are occupied and the lattice vibration in the planes has a much stronger effect. Each bond of MgB_2 gives superconductivity with individual characteristics, for example σ bonds are anisotropic and strongly coupled with the optical phonon mode,and it gives a large superconducting gap which consist of electrons and holes, $\triangle_\pi \approx 7meV$. The π-bonds are mostly electron-like and weakly couple with phonons, and it originates a low energy gap which consist of holes,$\triangle_\pi \approx 2meV$.$\sigma$-band gives $\kappa = 4(> \frac{1}{\sqrt{2}})$ and π-band gives $\kappa = 0.7(< \frac{1}{\sqrt{2}})$. But both gaps disappear at the same critical temperature . We have seen in subsection (1.4) different parameters which take place in this system with short physically meaning. MgB_2 is the superconductor used in this thesis.

1.7 The Bean model

Most of the properties of superconductors are reversible. There are other properties that are irreversible in the sense that when a parameter such as temperature, pressure, strength of applied electric or magnetic field changes in direction the system does not reverse, but hysteric effects occur. The vortices driven into the superconductor by an applied field or current, don't reach their equilibrium position because of their interactions with defects in the crystal lattice [17].

Bean's critical model, introduced by C.P Bean in 1962, gives a macroscopic explanation of the irreversible magnetization behaviour. It has proved to be a highly effective way to describe the macroscopic electrodynamic behaviour of superconductors without considering the vortex lattice in all its microscopic detail. The model assumes that wherever the current flows, it flows at the critical density and that the internal magnetic field is given by Maxwell equation as described in chapter 2. The model provides a phenomenological description for the hysteretic magnetization of type-II superconductors in a temporally varying applied field. The vortices start to penetrate into superconductor and they are pinned on the surface. In the area below the surface, which is penetrated by the vortices, a current density j_c flows. In others word, the material can only carry a limited current, the critical current j_c, in the presence of a magnetic field. This critical current will always flow where field has penetrated.

The magnitude of the critical current density is fixed by the characteristics of the particular superconductor, and it depends on such factors as the superconducting material, twinning, concentration of defect centers, etc. The internal magnetic field is given by Maxwell curl equation. There are two cases, the low-filed and High-field case. These two may be related in terms of a characteristic field proportional to the radius a , as given by

$$B^* = j_c \mu_0 a \tag{12}$$

B^* has the property that when the applied field $B_{app} = B^*$ the fields and currents are able to reach the center of the superconducting sample(see fig.5.b). Thus there are two cases, one for small applied field $B_{app} < B^*$ and the other for high applied fields $B_{app} = B^*$(see fig.5).

At low filed case, the vortices do not reach the inner surface and the interior stays field-free, whereas at high field, vortices penetrate the whole sample and a magnetic field appears in the interior, which then increases with increasing applied field [see fig.5].One can show that at high field the currents and the magnetic field are given by the expressions:

$$j_y(x) = j_c \qquad -a \leq x \leq 0, \tag{13}$$

$$j_y(x) = -j_c \qquad 0 \leq x \leq a, \tag{14}$$

$$B_z(x) = B_{app} - B^*(\frac{a+x}{a}) \qquad -a \leq x \leq 0, \tag{15}$$

$$B_z(x) = B_{app} + B^*(\frac{x-a}{a}) \qquad 0 \leq x \leq a. \tag{16}$$

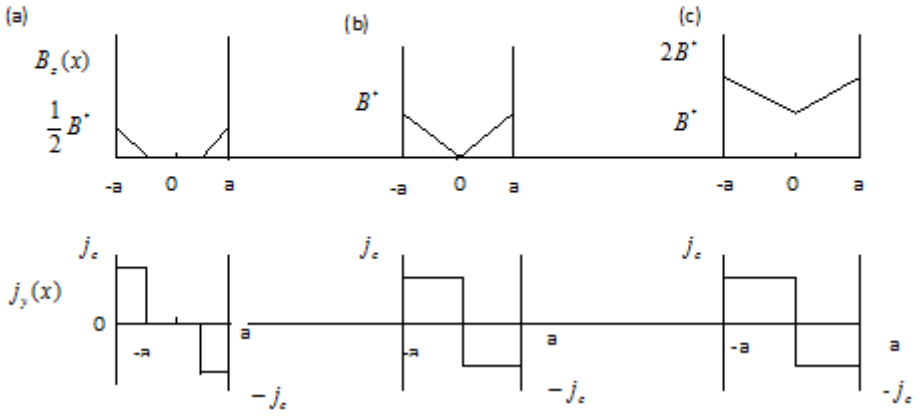

Figur 5: *Dependence of the internal field* $B_z(x)$ *, current density* $j_y(x)$ *and applied field given by: (a)*$\frac{B_{app}}{\mu_0 j_c a} = \frac{1}{2}$*,(b)*$\frac{B_{app}}{\mu_0 j_c a} = 1$*, and (c)*$\frac{B_{app}}{\mu_0 j_c a} = 2$ *. This and subsequent figures are drawn for the Bean model from [40].*

1.8 Road-map

This work is divided by five main parts.

a) *Basics equations that describe the method used to study thermomagnetic instability in SC.*This is the topic in chapter 2. The linearization of thermal equations and Maxwell equations for electromagnetic are treated. They lead to a quadratic equation. Hence, the quadratic, will be used to determine whether the system reach the instability.

b) *Suppression of thermo-magnetic instability in superconductors without deposed metals.* This is the topic in Chapter 3. The quadratic equation which describes whether the system is unstable or stable. Similarly result was found in Rakhmanovs paper [1]. However, it slightly deviates with Rakhmanovâs paper as a new parameter β is added in the calculation. The thermomagnetic instability due to thermal contact is studied.

c) *Suppression of thermo-magnetic in superconductors with deposed metal* . This is the topic in chapter 4. The study of flux jumps in superconducting sample coated with metal is investigated. To study the thermomagnetic instability due to the electrodynamic braking rather than thermal contact from recently experiment result[49], a model is built. This simple model is based on Gurevichs and Mints paper [3]. It leads to the results that confirm greatly the electrodynamic braking as origin for suppression of avalanches in superconductor with deposited metal.

d) *Onset/Offset of oscillations.* Chapter 5 is considered as an extra part of thesis. It concerns the imaginary solutions of dispersion equation for increment of instability. That describes the onset/offset of oscillations.

e) *Main conclusions* Chapter 6.

.

Chapter 2

2 Linearised equation for thermomagnetic instability

2.1 Sample geometry

The conventional theory of the thermomagnetic instability predicts "uniform" flux jump, where the flux front is essentially flat. But numerous magneto-optical studies have showed that the thermomagnetic instability in thin superconductor results in dendritic flux patterns [7],[1],[8]. This dendritic flux forms narrow "fingers" [see Fig.1].

In the present work the spatial pattern instability in bulk superconductors is investigated using the conventional approach- linear analysis of a set of differential equations describing small perturbations in the electric field E and in the temperature T. We assume that $\nabla \bullet \vec{j} = 0$ since we have the continuity of the current. To find the temperature and the electric field in superconducting sample the second Maxwell equation $\dot{\vec{B}} = -\nabla \times \vec{E}$ and the thermal equation $C\dot{T} = \kappa \bigtriangledown^2 T + \vec{j}E$ will be used respectfully. My work will be the study of instability in a superconducting slab placed in a parallel magnetic field (see Fig.6) and its suppression in steak of superconducting slabs and metals. In figure.6 the slab fills the semi-space $x > 0$,and the external magnetic field $\vec{H}$ is parallel to the$z$-axis so that the screening current $\vec{j}$ flows along y-axis.

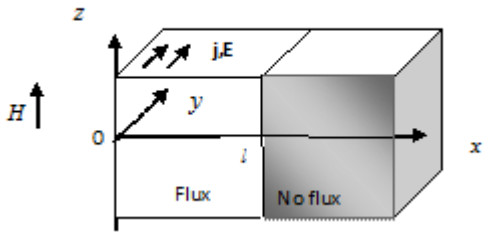

Figur 6: *Superconductor geometry without metal coating*

2.2 Basic Equation

To describe the flux jump instability in Superconductor slab, the sample is placed in a parallel magnetic field, $\vec{H}$. When this magnetic field is applied in the direction of the z-axis, the screening current **j** and the electric field **E** are induced inside the slab along the y-axis. For this geometry (see fig 6), the current J and magnetic field contributions in the sample (flux penetrated region $0 < x < l$) are described by the following Maxwell equation,

$$\bigtriangledown \times \vec{B} = \mu_0 \vec{J}, \qquad \vec{B}|_{x=0} = \mu_0 \vec{H} \tag{17}$$

Where the common approximation $\vec{B} = \mu_0 \vec{H}$ is used because $H_{c1} = 0$.

In this model, a linear analysis will be used to describe the small perturbations in the electric field E and temperature T . We allow the perturbations to vary in any direction, i.e., parallel and

perpendicular to the direction of the background current j and field E. Taking that in consideration, it will be able to determinate the stability and the instability build-up time.

The goal here is to find the quadratic equation [see subsec.'1.8']. First, let start with the case of studying thermo-magnetic in superconductor sample without metal coating. It will later become clear that thermal diffusion plays an important role in appearing for finger structure. Consequently, the electro-dynamic boundary conditions will be imposed. In type-II superconductors $j(E)$ is strongly non-linear, but for simplicity the corresponding Bean model is used.

Also, any B dependence of the critical current density is neglected. The exact form of the current-voltage curve,

$$\vec{j} = j(T, E)(\frac{\vec{E}}{E}) \tag{18}$$

is not crucially important. The point is that $E(j)$ curve is very steep such that its logarithmic derivative is very large. The relationship between the electrical conductivity and the differential conductivity gives us as function of electric field. The electrical conductivity is known as $\sigma_1 = \frac{j}{E}$. The differential conductivity is an important formula in our thesis and it is defined as

$$\sigma \equiv \frac{\partial j}{\partial E} \tag{19}$$

We define now $n(E) = \frac{\sigma_1}{\sigma} \equiv \frac{j}{\sigma E}$, where σ is the differential conductivity and σ_1 the electrical conductivity.
We mentioned above that $j(E)$ is strongly nonlinear in type-II superconductors. Nonlinearity implies that $\frac{\partial j}{\partial E} \neq \frac{j}{E}$ and it is valid for any conductors, both without or with metal coating. It follows from symmetry considerations that $E_x = 0$,while for the perturbation δE both components of this perturbations in x-and y-directions do not vanish.

2.3 Perturbation Analysis

2.3.1 Linearisation of dimensionless equation

In this section, the meaning is to find the dispersion equation for $\lambda(k_x, k_y)$. We will start with a linear analysis of a set of differential equations describing small perturbations in the electric field $\vec{E}$ and temperature T. Those linear differential equations will be inserted into Maxwell equations and thermal diffusion equation such that it leads us to the dispersion equation for λ.

In this way we determine the stability criteria in superconducting bulk. Also the interpretation of this dispersion relation is following:for $Re\lambda > 0$ the system is unstable,and for $Im(\lambda) \neq 0$ the system has oscillations.

The solutions of the equations above in subsection (2.2) can be represented in form

$$T + \delta T(x, y, z, t), E + \delta E(x, y, z, t), j + \delta j(x, y, z, t) \tag{20}$$

where T,E and j are background values.

The background electric field may be created by ramping the external magnetic field H,and we assume it to be coordinate independent even if in practice E is non-uniform.

We seek the perturbations in the form:

$$\delta T = \theta exp(\lambda t + ik_x x + ik_y y), \delta E_{x,y} = \varepsilon_{x,y} exp(\lambda t + ik_x x + ik_y y), \tag{21}$$

Where $\theta, \varepsilon_{x,y}$ are Fourier amplitudes and $Re(\lambda)$ is the dimensionless instability increment.

The wave numbers k_y and k_x characterize the scale of the perturbation along the y and x axes, respectively. We assumed (see the fig.6) infinite in the y direction,the k_y is arbitrary,while k_x can be limited by the width of the flux penetrated region and the boundary conditions.

The linearization of the current-voltage relation, Eq.(18) yields (see Appendix B)

$$\delta\vec{j} = \left(\frac{\partial j_c}{\partial T}\delta T + \sigma\delta E\right)\frac{\vec{E}}{E} + j_c\left(\frac{\delta\vec{E}}{E} - \frac{\vec{E}}{E^2}\right) \tag{22}$$

Where the electric conductivity$\sigma = \frac{j}{nE}$.

Similarly, the linear equations of Maxwell yields

$$\bigtriangledown \times \vec{B} = \mu_0 \delta\vec{J}, \tag{23}$$

$$\bigtriangledown \times \vec{E} = -\frac{\partial\vec{B}}{\partial t} \tag{24}$$

In the same way we can do the linearization of the thermal diffusion and we assume the current conservation $\nabla \cdot \vec{j} = 0$. The current conservation belongs to electromagnetics and the thermal diffusion is,

$$C\dot{T} = \kappa \bigtriangledown^2 T + \vec{j}E \tag{25}$$

where the first term to left of equation is the heat diffusion and second term is joule heating.

2.3.2 Calculations

We can now use equation (22) to find out δj_x and δj_y by taking in account that as showed in appendix (A):

$$\delta j_x = j_c\frac{\delta E_x}{E} \qquad , \delta j_y = \left(-|\frac{\partial j_c}{\partial T}| + \sigma\delta E\right) \tag{26}$$

Using equation (25), one can find δE_x. Also,from $\nabla \cdot \delta\vec{j} = 0$,we have $k_x\delta j_x + k_y\delta j_y = 0$.If one insert equation (26) into it one get $k_x j_c\frac{x}{E} = -k_{yy}$, which gives

$$\delta E_x = -\frac{k_y E\delta j_y}{k_x j_c} \tag{27}$$

To find the quadratic equation with variable λ, we will use the linearization of Maxwell equation (23), (24) and thermal equation (25), and it was previously assumed that the applied magnetic field is in z-direction.[see fig.6]
* We start first with$\bigtriangledown \times \vec{B} = \mu_0\delta\vec{J}$ and we have

$$\nabla \times \delta\vec{B} = \begin{vmatrix} \widehat{x} & \widehat{y} & \widehat{z} \\ \partial_x & \partial_y & \partial_z \\ 0 & 0 & \delta B_z \end{vmatrix} = (\partial_y\delta B_z, -\partial_x\delta B_z, 0) = \mu_0\delta\vec{j} \tag{28}$$

Due to the boundary condition, we have

$$-\frac{\partial \delta B_z}{\partial x} = \mu_0 \delta j_y \tag{29}$$

$$-ik_x \delta B_z = \mu_0 \delta j_y \tag{30}$$

$$\delta \dot{B}_z = -\frac{\mu_0}{ik_x} \lambda \delta j_y \tag{31}$$

Secondly we use $\bigtriangledown \times \vec{E} = -\frac{\partial \vec{B}}{\partial t}$ and we have

$$-\frac{\partial \vec{B}}{\partial t} = \nabla \times \delta \vec{E} = \begin{vmatrix} \widehat{x} & \widehat{y} & \widehat{z} \\ \partial_x & \partial_y & \partial_z \\ \delta E_x & \delta E_y & 0 \end{vmatrix} \tag{32}$$

$$\delta \vec{B_z} = -\frac{\partial \delta E_y}{\partial x} + \frac{\partial \delta E_x}{\partial y} \tag{33}$$

if we put equation (31) equals (33), and it gives

$$\frac{\partial \delta E_y}{\partial x} - \frac{\partial \delta E_x}{\partial y} = \frac{\mu_0}{ik_x} \lambda \delta j_y \tag{34}$$

Since we know $\delta E_y, \delta E_x$ and δj_y,their derivations in equation(34) gives us

$$k_x \delta E_y = \frac{\mu_0}{k_x} \lambda \delta j_y - \frac{k_y^2 E}{j_c} |\frac{\partial j_c}{\partial T}| \delta T + \frac{k_y^2 E \sigma}{k_x j_c} \delta E_y \tag{35}$$

Set δj_y inn and separate δE_y and δT term,it gives

$$\left(-k_x - \frac{\mu_0 \sigma}{ik_x} \lambda - \frac{k_y^2 j}{k_x n j_c} \right) \delta E_y = \left(-\frac{\mu_0}{k_x} |\frac{\partial j_c}{\partial T}| \lambda - \frac{k_y^2 E}{k_x j_c} |\frac{\partial j_c}{\partial T}| \right) \delta T \tag{36}$$

This is the result from electrodynamics and it satisfies my expectation since i want to have it in separated terms δE_y and δT. The next step will be to use the thermal diffusion (25) such that it gives us an equation with separate δE_y and δT terms as above. Let start with it,

$$C\dot{T} = \kappa \bigtriangledown^2 \delta T + j \delta E + \delta j E \tag{37}$$

We separate δE_y andδT term in Fourier space and it gives

$$C\lambda \delta T = -\kappa \left(k_x^2 + k_y^2 \right) \delta T + j \delta E_y + \delta j_y E_y \tag{38}$$

$$\left(C\lambda + \kappa \left(k_x^2 + k_y^2 \right) - \frac{\partial j_c}{\partial T} E \right) \delta T = \left(\frac{j}{n} + j \right) \delta E_y \tag{39}$$

We have now from equation (36) and (39)$A\delta E_y = B\delta T$ and $F\delta E_y = D\delta T$ where

$$A = \left(\frac{\mu_0 \sigma}{k_x} \lambda + \left(k_x + k_y^2 \frac{j}{k_x n j_c} \right) \right) \tag{40}$$

$$B = \left(\frac{\mu_0}{k_x} |\frac{\partial j_c}{\partial T}| \lambda + k_y^2 \frac{E}{k_x j_c} |\frac{\partial j_c}{\partial T}| \right) \tag{41}$$

$$D = \left(\frac{1}{n} + 1 \right) j, \tag{42}$$

$$F = \left(C\lambda + \kappa \left(k_x^2 + k_y^2 \right) - \frac{\partial j_c}{\partial T} E \right) \tag{43}$$

Using $AD\delta E_y \delta T = BF\delta E_y \delta T$, it can help us to find the dispersion equation for λ,

$$\left[\frac{\mu_0 \sigma}{k_x} \lambda + \left(k_x + \frac{k_y^2 E \sigma}{k_x j_c} \right) \right] + left[c\lambda + \kappa(k_x^2 + k_y^2) + |\frac{\partial j_c}{\partial T}|E\,)] = \left[\frac{\mu_0}{k_x} |\frac{\partial j_c}{\partial T}| \lambda + \frac{k_y^2 E}{k_x j_c} |\frac{\partial j_c}{\partial T}| \right] \left[\frac{j}{n} + j \right] \tag{44}$$

This gives

$$\frac{c\mu_0\sigma}{k_x}\lambda^2 + \left(\frac{c\mu_0\sigma}{k_x}\kappa(k_x^2+k_y^2) + \frac{c\mu_0\sigma}{k_x}\frac{\partial j_c}{\partial T}E + ck_x + \frac{ck_y^2 j}{k_x n j_c} - \frac{\mu_0 j}{k_x n}|\frac{\partial j_c}{\partial T}| - \frac{\mu_0 j}{k_x}|\frac{\partial j_c}{\partial T}| \right)\lambda + k_x\kappa(k_x^2+k_y^2) + k_y^2\frac{j\kappa(k_x^2+k_y^2)}{k_x n j_c}k_x E|\frac{\partial j_c}{\partial T}| + k_y^2\frac{jE}{k_x n j_c}|\frac{\partial j_c}{\partial T}| - \frac{k_y^2 E j}{k_x}|\frac{\partial j_c}{\partial T}| = 0 \tag{45}$$

we multiply this equation by $\frac{k_x}{C\mu_0\sigma}$

$$\lambda^2 + \frac{1}{c}\left(\kappa(k_x^2+k_y^2) + |\frac{\partial j_c}{\partial T}|E \right)\lambda - \frac{E}{c}|\frac{\partial j_c}{\partial T}|\lambda - \frac{j}{c}|\frac{\partial j_c}{\partial T}|\lambda + \frac{k_x}{\mu_0\sigma}\left(k_x + \frac{k_y^2\sigma}{k_x j_c} \right)\lambda + \frac{k_x}{c\mu_0\sigma}\left(\kappa(k_x^2+k_y^2) + E|\frac{\partial j_c}{\partial T}| \right) - \frac{k_x}{c\mu_0\sigma}\left(\frac{k_y^2 E}{k_x j_c}|\frac{\partial j_c}{\partial T}| \right)(E\sigma) - \frac{k_x}{c\mu_0\sigma}\left(\frac{k_y^2 E}{k_x j_c}|\frac{\partial j_c}{\partial T}| \right)(j) = 0 \tag{46}$$

$$\lambda^2 + \left(\frac{\kappa}{c}(k_x^2+k_y^2) - \frac{j}{c\sigma}|\frac{\partial j_c}{\partial T}| + \frac{k_x^2}{\mu_0\sigma} + \frac{k_y^2 E}{\mu_0 j_c} \right)\lambda + k_x^2\frac{\kappa(k_x^2+k_y^2)}{c\mu_0\sigma} + \frac{E}{c\mu_0\sigma}|\frac{\partial j_c}{\partial T}| + k_y^2\left(\frac{E\kappa(k_x^2+k_y^2)}{c\mu_0 j_c} - \frac{E^2 n}{c\mu_0}|\frac{\partial j_c}{\partial T}| \right) = 0 \tag{47}$$

We can write it in quadratic equation

$$\lambda^2 + P\lambda + Q = 0 \tag{48}$$

Where

$$P = \left(\frac{\kappa}{c}(k_x^2+k_y^2) - \frac{j}{c\sigma}|\frac{\partial j_c}{\partial T}| + \frac{k_x^2}{\mu_0} + \frac{k_y^2 E}{\mu_0 j_c} \right) \tag{49}$$

$$Q = k_x^2\left(\frac{\kappa}{c\mu_0\sigma}(k_x^2+k_y^2) + \frac{E}{c\mu_0\sigma}|\frac{\partial j_c}{\partial T}| \right) + k_y^2\left(\frac{E\kappa(k_x^2+k_y^2)}{c\mu_0 j_c}\frac{E^2 n}{c\mu_0}|\frac{\partial j_c}{\partial T}| \right) \tag{50}$$

2.3.3 Dimensionless Parameters

In this subsection, dimensionless parameters are induced such that it leads to a simple form for dispersion relation we are looking for. One will observe that an extra parameterβ , compared to the quadratic equation in [1], will be added during the calculation.
This extra parameter has scale length b which is similar to w in [1] defined as

$$w^2 = \frac{CT_c}{\mu_0 j_c^2} \tag{51}$$

Let now those two parameters τ and β be defined as $\tau = \frac{\sigma\kappa\mu_0}{C}$ and $\beta = \frac{b^2 j_c |\frac{\partial j_c}{\partial T}|\mu_0}{C}$ such that

$$\kappa = \frac{\tau C}{\sigma\mu_0} \tag{52}$$

and

$$|\frac{\partial j_c}{\partial T}| = \frac{\beta C}{b^2 j_c \mu_0} \tag{53}$$

We include them in the quadratic equation (48) and it gives

$$\lambda^2 + \left[\frac{\tau(k_x^2+k_y^2)}{\mu_0\sigma} - \frac{\beta j}{\mu_0\sigma b^2 j_c} + \frac{k_x^2}{\mu_0\sigma} + \frac{k_y^2 E}{\mu_0 j_c}\right]\lambda + k_x^2\left[\frac{\tau(k_x^2+k_y^2)}{(\mu_0\sigma)^2} + \frac{\beta E}{\mu_0^2 b^2 j_c \sigma}\right] + k_y^2\left[\frac{\tau(k_x^2+k_y^2)nE^2}{\mu_0^2 b^2 j_c^2}\right] = 0 \tag{54}$$

We want to induce a characteristic time, $t_0 = \frac{\mu_0 b^2}{\rho_0}$ such that $\tilde{\lambda} = t_0\lambda$ If $\tilde{k}_x = bk_x$ and $\tilde{k}_y = bk_y$, where b is some length, one obtains quadratic equation:

$$\tilde{\lambda^2} + t_0 P\tilde{\lambda} + t_0^2 Q = 0 \tag{55}$$

$$\tilde{\lambda}^2 + \left[\frac{\mu_0 b^2}{\rho}\frac{\tau(\tilde{k}_x^2+\tilde{k}_y^2)}{\mu_0\sigma} - \frac{\mu_0 b^2}{\rho_0}\frac{\beta j}{\mu_0\sigma b^2 j_c} + \frac{\mu_0 b^2}{\rho_0}\frac{k_x^2}{\mu_0\sigma} + \frac{\mu_0 b^2}{\rho_0}\frac{k_y^2}{\mu_0\sigma}\right]\lambda + k_x^2\left[\frac{\mu_0 b^2}{\rho_0}\frac{\tau(k_x 2+k_y^2)}{\mu_0^2\sigma^2} - \frac{\mu_0 b^2}{0}\frac{\beta E}{\mu_0^2 b^2 j_c\sigma} + k_y^2\left[\frac{\mu_0 b^2}{\rho_0}\frac{nE\tau(k_x 2+k_y^2)}{\mu_0^2\sigma j_c} + \frac{\mu_0 b^2}{\rho_0}\frac{\beta E}{\mu_0^2 b^2 j_c^2}\right] = 0 \tag{56}$$

$$\tilde{\lambda}^2 + \frac{1}{\rho_0\sigma}\left[\tau(\tilde{k}_x^2+\tilde{k}_y^2 - \frac{\beta j}{j_c} + \tilde{k}_x^2 + \frac{\tilde{k}_y^2 j}{nj_c}\right]\tilde{\lambda} + \frac{1}{(\rho_0\sigma)^2}\tilde{k}_x^2\left[\tau(\tilde{k}_x^2+\tilde{k}_y^2) + \frac{\beta j}{nj_c}\right] + \frac{1}{\rho_0\sigma}\tilde{k}_y^2\left[\frac{En\tau(\tilde{k}_x^2+\tilde{k}_y^2)}{j_c} - \frac{\beta j^2}{nj_c^2}\right] = 0 \tag{57}$$

Let $\alpha = \rho_0\sigma$ we can write this new quadratic equation in this form:

$$\alpha^2\tilde{\lambda}^2 + \left[\tau(\tilde{k}_x^2+\tilde{k}_y^2) - \frac{\beta j}{j_c} + \tilde{k}_y^2\frac{j}{nj_c}\right]\alpha\tilde{\lambda} + \tilde{k}_x^2\left[\tau(\tilde{k_x^2}+\tilde{k_y^2}) + \frac{\beta}{nj_c}\right] + \tilde{k}_y^2\left[\frac{\tau(\tilde{k}_x^2+\tilde{k}_y^2)j}{nj_c} - \frac{\beta j^2}{nj_c^2}\right] = 0 \tag{58}$$

2.4 The dispersion relation for $\tilde{\lambda}$

We have found a new quadratic equation which is similar to equation(20)in Rakhmanovs paper[1]. The main point in this quadratic equation compared to the one in [1], has a new parameter β :

$$\beta = \frac{b^2 j_c |\frac{\partial j_c}{\partial T}| \mu_0}{C} \tag{59}$$

This extra parameter is important for dispersion relation because we want b to be temperature independent. When b is fixed, it means that β is fixed. In paper [1], the writers assumed it to be 1.

But we want to add this new parameter such that we can study what happens with thermomagnetic instability or what are physical behaviour when the parameterβ is no longer 1 and it can vary, decreasing or increasing. The new quadratic or dispersion relation for$\tilde{\lambda}$ is

$$\alpha^2 \tilde{\lambda}^2 + P\alpha\tilde{\lambda} + Q = 0 \tag{60}$$

where

$$P = \tilde{k}_x^2 + \frac{\tilde{k}_y^2}{n}\frac{j}{j_c} - \beta\frac{j}{j_c} + \tau(\tilde{k}_x^2 + \tilde{k}_y^2) \tag{61}$$

$$Q = \tau\left(\tilde{k}_x^4 + \frac{n+1}{n}\tilde{k}_x^2\tilde{k}_y^2\frac{j}{j_c}\right) + \frac{\beta}{n}\left(\tilde{k}_x^2 - \tilde{k}_y^2\frac{j}{j_c}\right)\frac{j}{j_c} \tag{62}$$

Thesis focuses only on $\Re(\tilde{\lambda}) > 0$ and $\Re(\tilde{\lambda}) < 0$,therefore we choose $\alpha = 1$. We defined in previous chapter (equ.[52][53]) that these two parameters as: $\tau = \frac{\sigma\kappa\mu_0}{C}$ and $\beta = b^2 j_c \mu_0 \frac{|\partial j_c}{\partial T} C$ where σ is the electric conductivity,C is the specific heat capacity, ρ_0 is the resistance, μ_0 is the permeability, j_c is the critical current density and κ is the thermal conductivity.

The system is unstable if $\Re\tilde{\lambda}(k_x, k_y) > 0$

.

Chapter 3

3 Thermomagnetic instability in bulk superconductor without metal coating

3.1 Thermal contact

The avalanches extends the physical picture of the critical state description presented in previous chapter. Under certain conditions, the instability develops into a flux jumps. I was mentioned in introduction section that these instabilities were already subject of many studies in the early 1960 [21].

Thermo-magnetic instability has been explained to be origin of flux jumps by Bean [40], Mints and Rakmanov [2], and others. Qualitatively the idea involves two main observations[4]:
(i) motion of magnetic flux releases energy and hence increases the local temperature; and (ii) the temperature rising decreases flux pinning, and hence facilitates the flux motion.

The conventional theory of the thermo-magnetic instability[2], [22]predicts "uniform" flux jumps, when the flux front is essentially flat. In this chapter the spatial patterns of the instability in bulk superconductor is studied using the conventional approach presented in previous chapter- linear analysis of set of differential equations describing small perturbations in the electric field E and temperature T. This approach leads to a dispersion equation (60) that determines whether the system is unstable (assuming $\alpha = 1$, n is a constant and $j = j_c$):

$$\tilde{\lambda}^2 + P\tilde{\lambda} + Q = 0 \tag{63}$$

where

$$P = \tilde{k}_x^2 + \frac{\tilde{k}_y^2}{n} - \beta + \tau(\tilde{k}_x^2 + \tilde{k}_y^2) \tag{64}$$

$$Q = \tau\left(\tilde{k}_x^4 + \frac{n+1}{n}\tilde{k}_x^2\tilde{k}_y^2\right) + \frac{\beta}{n}\left(\tilde{k}_x^2 - \tilde{k}_y^2\right) \tag{65}$$

The solutions to this equation are:

$$\tilde{\lambda}_1^2 = \frac{-P + \sqrt{P^2 - 4Q}}{2} \tag{66}$$

$$\tilde{\lambda}_2^2 = \frac{-P - \sqrt{P^2 - 4Q}}{2} \tag{67}$$

The flux jumps depends on several material parameters [see subsection 1.4]. There are two important parameters which are useful in study of thermo-magnetic instability- parameter τ and β. The first one,τ, is the ratio of thermal and magnetic diffusion coefficients. The another one,β, is the characteristic perturbation from external source. In next subsection, their definition and estimation of maximum and minimum values will be presented.

3.2 The key dimensionless parameters

β and τ are the key dimensionless parameters for thermo-magnetic model. One sees in Equ.(52) that β is a function of temperature T and τ is a function of electric field E. They are useful for studying instability under dependency of increasing/decreasing temperature, magnetic field or electric field. Their maximum and minimum values can be estimated(with values of Table.1): (i) Parameter β is the characteristic perturbation from external source ,and it is defined in (53) as

$$\beta = \frac{b^2 j_c \mu_0 |\frac{\partial j_c}{\partial T}|}{C} \tag{68}$$

where b is the characteristic length for adiabatic instability. Assume that b is fixed, one can estimate the maximum and minimum of parameter β since it is a function of temperature. Also, one can derive it with temperature T and put it equal zero. This is the analytic way to find his max/min and using values from Table.1, it gives

$$\beta_{max} = \frac{(0.02)^2(10^{11})(4\pi)(10^{-7})(10^{10})(\frac{T}{T_c})^{-3}}{3500} \approx 4.8(\frac{T}{T_c})^{-3} \tag{69}$$

$$\beta_{min} = \frac{(6.6(10^{-6}))^2(10^{11})(4\pi)(10^{-7})(10^{10})(\frac{T}{T_c})^{-3}}{3500} \approx 0.02(\frac{T}{T_c})^{-3} \tag{70}$$

The plot of parameterβ as function of temperature T: Parameter β in Equ.(68)contains the cha-

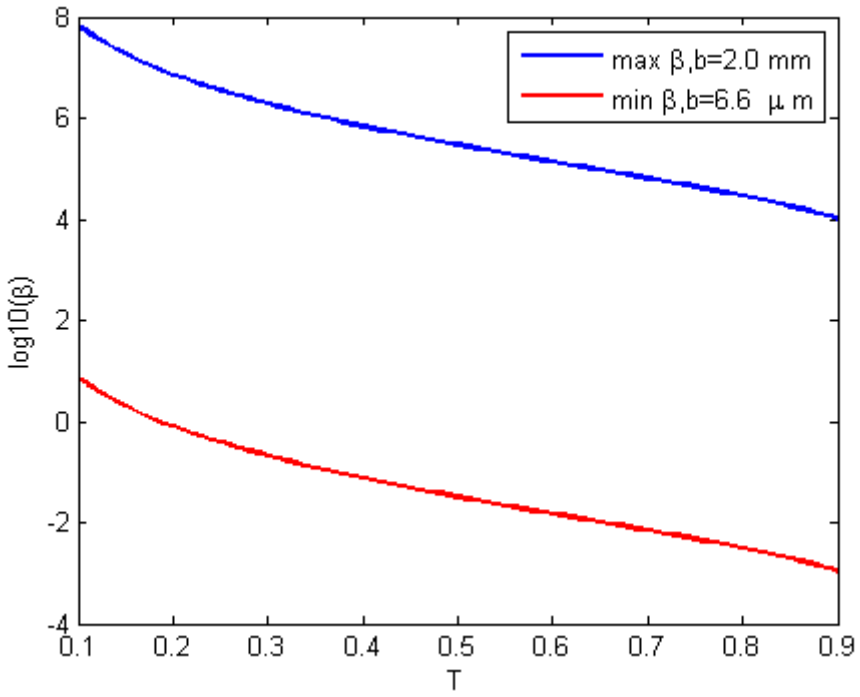

Figur 7: *The plot of parameter β as function of temperature T.β is max when the characteristic length scale b is max($b = 2mm$)and β is min when b is min($b = 6.6\mu m$) according to Equ.(68)*

racteristic length for adiabatic instability b which is proportional to inverse wave numbers that

characterize the scale for perturbation k_x and k_y. In thesis, the max $b = 2mm$ and the min $b = 6.6\mu m$. Beyond/under maximum/minimum of these values the dispersion equation (63) is meaningless.

(ii) Parameter τ is the ratio of thermal and magnetic diffusion coefficient, and it is defined as:

$$\tau = \frac{D_{th}}{D_m} = \frac{\kappa\mu_0\sigma}{C} \tag{71}$$

Where D_{th} is the thermal diffusion coefficient and D_m is the magnetic diffusion. The thermal diffusion coefficient is defined as the thermal conductivity divided by volumetric heat capacity(we assume this density equal 1) such that

$$D_{th} = \frac{\kappa}{C} \tag{72}$$

The magnetic diffusion coefficient is obtained by using power law and Maxwell equation. In Bean critical state model, the power law is defined as $\frac{E}{E_c} = \left(\frac{j}{j_c}\right)^n$. We saw previously that Bean model is only valid for equilibrium condition and satisfies the magnetic diffusion equation under the steady- state condition. Parameter τ is a function of electric field. The resistivity will increases with exponent in power law,therefore we choose a small n since we know that the magnetic diffusion coefficient is small because of low resistivity in the vicinity $j = j_c$[see details in Appendix G]. For the Bean model, the minimum electric field $E_{min} = \dot{B}_c b(\approx 10^{-5}V/m)$ and the maximum electric field $E_{max} = \rho_0 j_{c0} = 7.10^3 V/m$,where ρ_0 is the resistivity and B_c is the critical magnetic field defined as $B_c = B_c(0)\left[1 - \left(\frac{T}{T_c}\right)^2\right]$, $B_c(0) = \mu_0\lambda j_c$ within the London depth λ_L and critical current density j_c.Using values from table.1 and from figure 8 above, one might estimate $\tau_{max} \approx 4.6.10^6$ and $\tau_{min} \approx 0.01$ according to equ.(71)

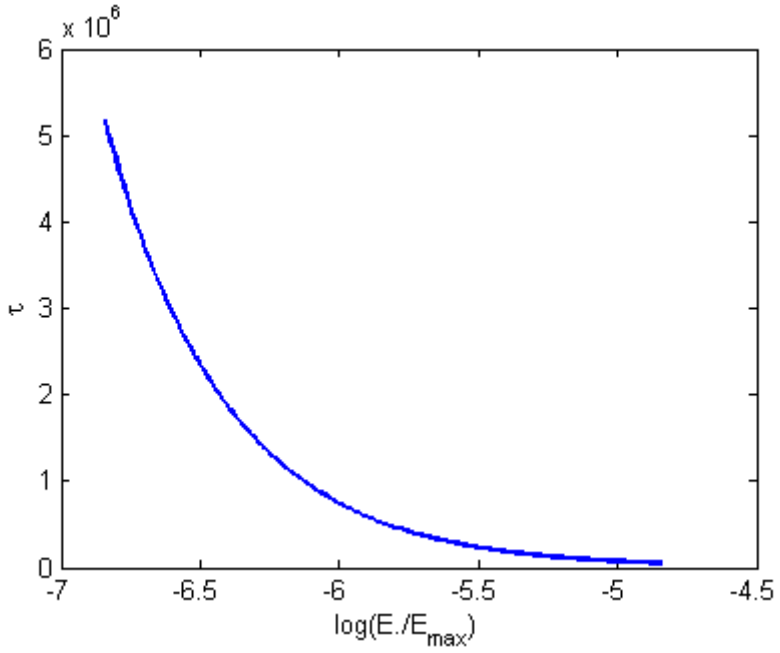

Figur 8: *The plot of parameter τ as function of electric field [log(E/E_{max})].τ is maximum when the electric field E is minimum($E = 10^{-5}V/m$)and τ is minimum when E is maximum($E = 7.10^3 V\ m$)according to Equ.(71).*

3.3 Result and discussion

The problem about the thermo-magnetic instability in superconducting sample without deposed metal is solved more exactly, and start by establishing the proper boundary conditions .

3.3.1 Boundary conditions

According to Equ.(70) small τ correspond to high electric field. It will be showed in later discussion that a finger structure may appear only for $\tau < 1$. It means that the magnetic diffusion is faster that thermal diffusion. Consequently, only the electrodynamic boundary condition is needed.

Also, the magnetic field has only z-component, and the first boundary condition is $\delta E_y = 0$,$x = 0$. It means that current does not flow across the superconductors surface,δj_x is proportional to $\delta E_x = 0$ at $x = 0$. The second condition is that $\delta E_y = 0$,$x = l$ where l is the flux penetration depth [see fig.6].

3.3.2 The physical interpretation of dispersion equation for $\tilde{\lambda}$

Many solutions come out from equations (66) and (67). My thesis is related to one of them, more precisely, there are two cases. The first one is the real part(when $P^2 > 4Q$) and the second one is the imaginary part(when $P^2 < 4Q$) and the onset/offset of instability (when $P^2 = 4Q$). Let start with the study of the system when the electric field is high and when it is low. It is known now from equation (71) the ratio of thermal and magnetic diffusion coefficient τ approaches zero with high electric field and vice versa.

Assume the real part solution of dispersion equation (63) when $P^2 > 4Q$, the parameter $\beta = 1$ and $j = j_c$(see Appendix F). The dispersion equation for λ becomes more transparent when the heat conductivity can be omitted, i.e, $\tau = 0$. Then

$$\lambda^2 + \lambda\left(k_x^2 + \frac{k_y^2}{n} - \beta\right) + \frac{\left(k_x^2 + k_y^2\right)}{n} = 0 \tag{73}$$

At $k_x = 0$ the system is always unstable(see fig.9.a,for $\tau = 0$). The reason is that there is a fixed transport current heating by the electric field under adiabatic condition. When the electric field increases or for high electric field the ratio τ becomes smaller. For perturbations uniform in y-direction($k_y = 0$) the instability develops only if $k_x < 1$. However if $k_y \to \infty$, then the system becomes unstable for all k_x and arrive at max growth rate, $\lambda = 1$.

The uniform mode of instability can be determined by checking[1] if the maximum real part of λ, note as λ_{max} in thesis,always corresponds to $k_y = 0$. However, for high electric field or small τ,λ_{max} can occur for a nonzero k_y. Moreover, it is possible that the system is stable with respect to uniform perturbations, while unstable for perturbations with finite k_y. This means that a non-uniform structure along the y-direction will be formed.Starting with very low electric field, the instability becomes uniform when the heat conductivity increases while it has non-uniform mode when the heat conductivity has a very small value close to zero. For small applied magnetic fields the system is stable. As the field increases, the flux penetration depth grows, and hence k_x goes down (see fig.9.b). It is clear that the instability range extends to large k_y for high electric field. Since λ_{max} always corresponds to $k_y = 0$, therefore we can argument that the instability develops in a uniform mode for relatively large τ.

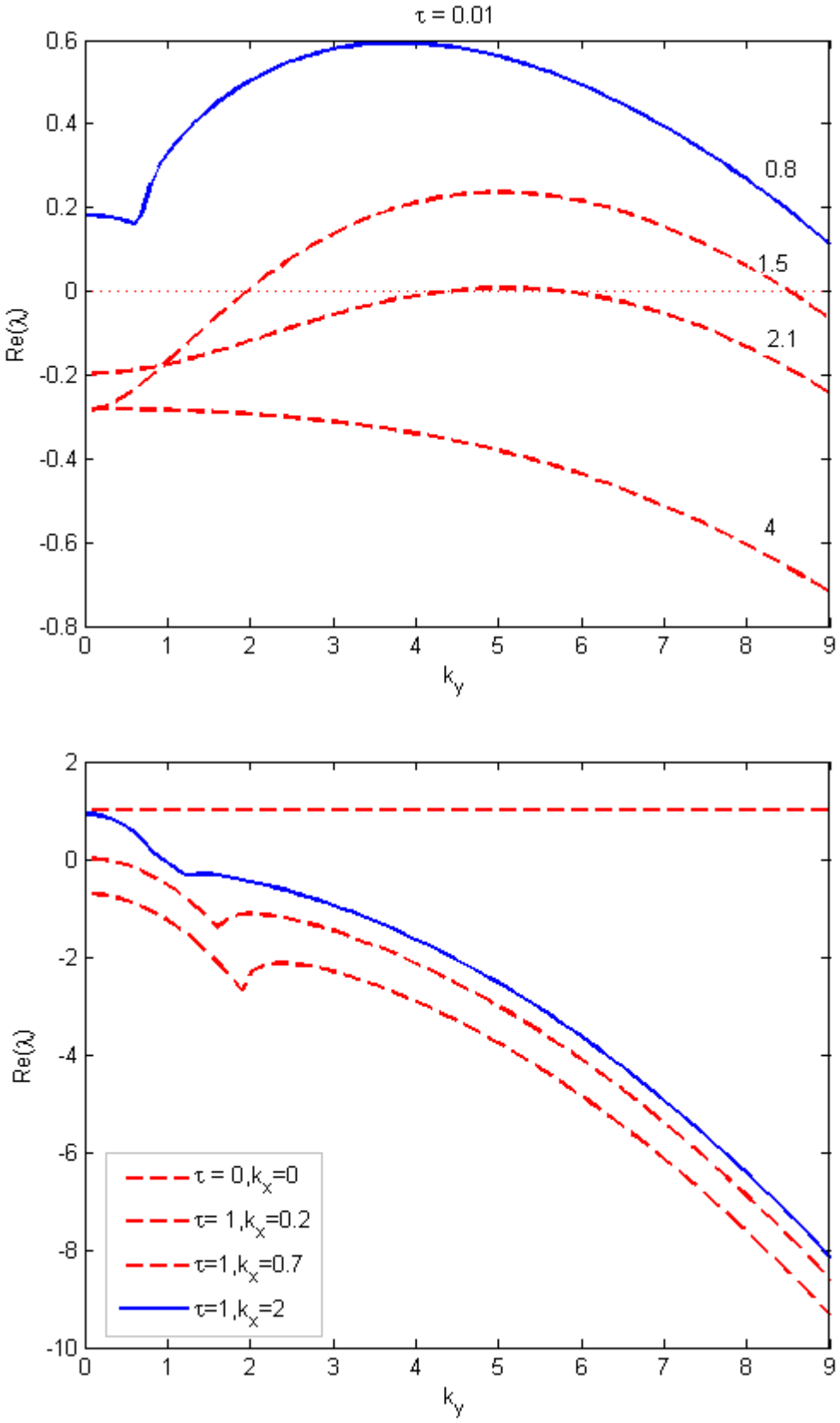

Figur 9: *The instability increment* $Re(\lambda)$ *found from Eq.(63) for* $n = 10$ *,*$\beta = 1$*,and different* k_x*: a. Slow heat diffusion,the maximal* $\Re(\lambda)$ *is at finite* k_y*. b.fast heat diffusion,*$\Re(\lambda)$ *corresponds to uniform perturbations(*$k_y = 0$*).*

The characteristic perturbation from external source β has proved to be a effective parameter in stabilizations process. It affects the system stability since it is connected to the temperature T through the critical current density j_c and to the wave numbers that characterize the scale for perturbation k_x and k_y.

Let assume that the size of the sample is fixed with k_x. The parameter β will depend only on temperature T. One expects that the system becomes more stable when β decreases. Thus, the system is always stable for $\beta = 0$. The physical reason might be the fact that β is related to the critical current density j_c. And when $T \approx T_c$ the sample is close to ohmic state since j_c decreases dramatically to zero. This process is available for uniform and non-uniform mode.[see fig.10] In

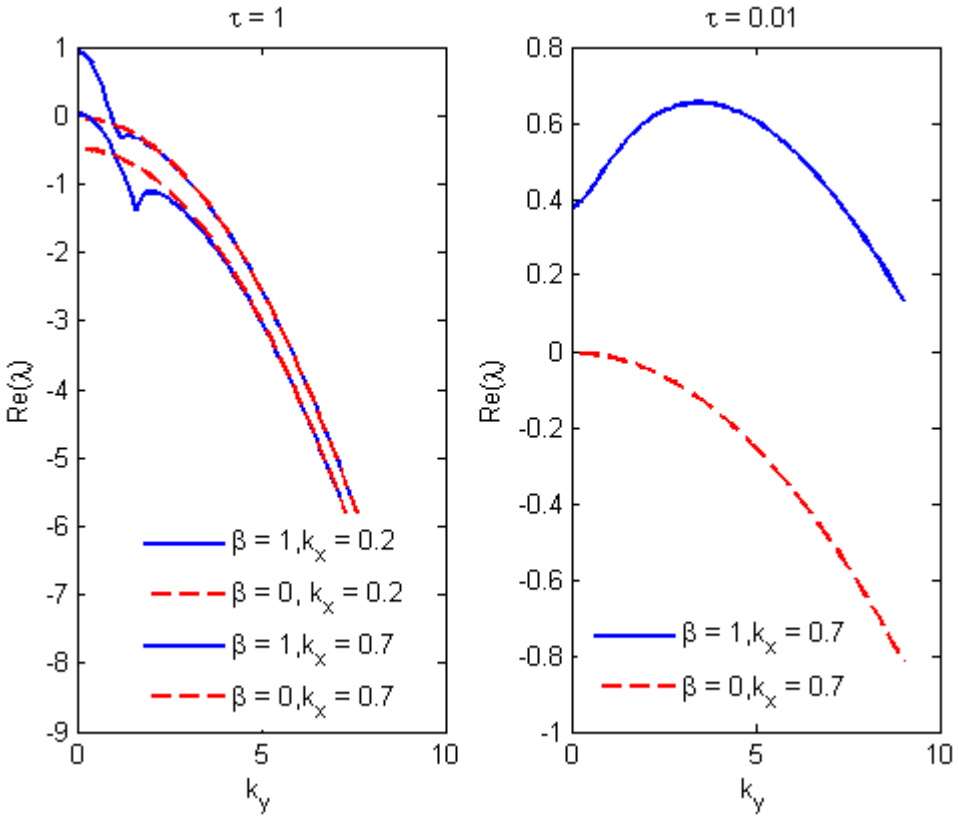

Figur 10: *The plot of increment $Re(\lambda(k_y))$ from Equ.(63) with different β. These plots show that the decreasing of parameter β stabilize the system.*

previous chapter one assumed that $\tilde{k}_{x,y} = bk_{x,y}$ such that $bk_{x,y} = \frac{2\pi}{l}b$. The maximum and minimum values are $b_{max} = 2mm$ and $b_{min} = 6.6\mu m$ respectively. It means that the largest $\tilde{k}$ that one can have is

$$\tilde{k}_{x,y} = \frac{2\pi}{b}b = 2\pi, \qquad l = b \tag{74}$$

and similar for smallest $\tilde{k}$

$$\tilde{k}_{x,y} = \frac{2\pi b}{1mm}, \qquad l = 1mm \tag{75}$$

where l is the flux penetration length.[see fig.6]

I mentioned above, parameter β is proportional to inverse $k_{x,y}$. It is obvious that the system

stabilizes when $k_{x,y}$ increases. In others word, larger $k_{x,y}$ corresponds to smaller β. The zero contour plot of maximum $Re(\lambda)$ or λ_max in parameters τ and β shows this effect[see fig.11]. The

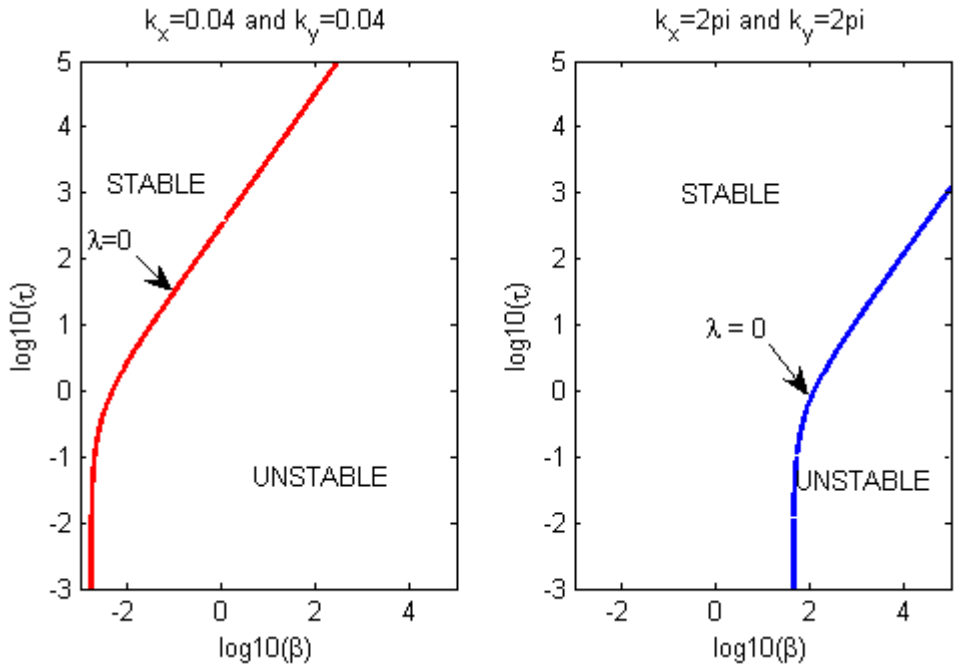

Figur 11: *The zero contour plot of max $Re(\lambda)$ in τ and β.The left side of $\lambda = 0$line is stable region and the right side is unstable region. The stability of system corresponds to increasing $k_{x,y}$ according to Equ.(68).*

red and the blue lines in zero contour plot above(see fig.11) correspond to the onset/offset of instability. These lines separate the stable and unstable regions. Analytically, it exist for solutions $P = 0$ where $P^2 < 4Q$, for $Q = 0$ when $P^2 > 4Q$ and finally when both P and Q are zeros. The another two cases $Re(\lambda) > 0$ and $Re(\lambda) < 0$ are summarized in Table.2 [see page 56]

3.4 Summary

The thermo-magnetic instability in superconductor is studied with linear stability analysis of heat diffusion and Maxwell equations. It leads to a dispersion equation that can be used to determine whether the system is unstable. The new dispersion equation is similar to dispersion equation from Rakhmanovs paper[1]. A new parameter,called β, is induced [21]. It characterises the perturbation from external source. Parameter β seems to stabilize the system when it decreases. The system becomes always stable when β reach zero. Parameter β, when the characteristic scale length for adiabatic instability b is fixed, is temperature dependent since it is proportional to the critical current density $j_c(T)$[see Equ.(68) and subsection 1.4].It is obvious to expect that the system stabilises when the temperature T decreases. Figure (10) is devoted to show the stabilisation of system with parameter β.

Both high electric field (corresponding to small parameter τ) and low electric field(corresponding to high parameter τ) background are exploited. The results show that the fingering instability occurs if the background of electric field is so high that magnetic flux diffusion proceeds much faster than the heat diffusion. This confirms that thermal conductor is the origin of flux jumps in superconducting sample.

.

Chapter 4

4 Suppression of thermomagnetic instability in bulk superconductor with metal coating

4.1 Magnetic braking

It was claimed in previous chapter that the thermal conduction is the suppression of flux jumps in superconductor [2],[6].Recently however, Fabiano and many others experiments[2], [3], [4], [9] have shown that the suppression of avalanches occurs even with no contact between the metal and superconducting sample.

It has been suggested that the stabilization of avalanches to a magnetic braking effect due to eddy currents generated in the added metal layer[49]. To shed light on this suggestion, a model is caring out that takes into account the deposed metal part on bulk superconductors.

4.2 Model for suppression of thermomagnetic instability with metal coating

In this subsection, the goal is to build a model for electrodynamic braking as a cause for suppression of avalanches with deposed metal. The model will lead to a new dispersion equation for $\tilde{\lambda}$ compared to equ.(63). The fraction of superconducting specimens is called x and for non-superconducting is $(1-x)$, for example metal [see fig.12]. It is a simple model that helps me to find the dispersion equation for $\tilde{\lambda}$ with metal coating. The principle of this model is based on an article written by Gurevich and Mints,[4]. In section "composite superconductors" from this article, they explained that the metal greatly reduces the thermal, electrodynamical, and mechanical instabilities characterizing hard superconductors. To avoid repeating calculations as i did in previous chapter, i used the superconductor-metal geometry as seen on figure 12.

The model has two conductors in parallel, one ohmic conductor and one superconductor, such that the total current density is defined as

$$j^{(1)} = \sigma^{(1)} E \tag{76}$$

where the total electrical conductivity $\sigma^{(1)} = x\sigma_s^{(1)} + \sigma_m^{(1)}(1-x)$.The superscript '$^{(1)}$' distinguishes the differential and non-differential conductivity. The differential conductivity is defined as $\sigma \equiv \frac{\partial(\sigma^{(1)}E)}{\partial E}$.

The electrical conductivity of superconductor is $\sigma_s = x\frac{\partial(\sigma_s^{(1)}E)}{\partial E}$ and the electrical conductivity of metal is $\sigma_m = (1-x)\frac{\partial(\sigma_s^{(1)}E)}{\partial E}$. The ratio between the electrical conductivity and its differential for superconductor is the parameter:

$$s = \frac{\sigma_s^{(1)}}{\sigma_s} \tag{77}$$

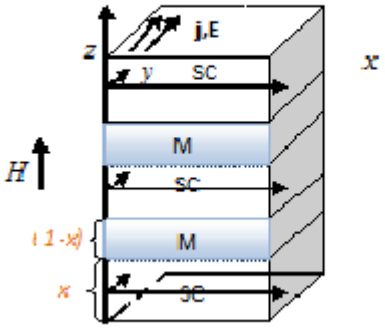

Figur 12: *Geometry of superconductors with deposed metals in sandwich form*

In previous chapter concerning thermo-magnetic instability without metal coating, the ratio (76) was called n and it was a constant. In present case, thermo-magnetic with deposed metal, the parameter n for total (superconductor and metal) is:

$$n = \frac{\sigma^{(1)}}{\sigma_s} \tag{78}$$

The electrical conductivity of metal σ_m is a constant. Let us recall the calculation of the differential electrical conductivity and it will helps to find the total current in (75). The calculation of the electrical conductivity in the superconducting sample leads to $\sigma_s^{(1)} = \sigma_0 \left(\frac{E}{E_0}\right)^{-\left(1-\frac{1}{S}\right)}$ (see Appendix D) such that the current density is defined through the superconducting sample (without deposed metal) as

$$j_s^{(1)} = \sigma_0 \left(\frac{E}{E_0}\right)^{-\frac{S-1}{S}} E \tag{79}$$

Derive (79) to find the differential conductivity in the case of non-metal coating,

$$\sigma_s = \frac{\partial j_s^{(1)}}{\partial E} = \frac{1}{s}\sigma_0 \left(\frac{E}{E_0}\right)^{\frac{1-S}{S}} = \frac{1}{s}\sigma_s^{(1)} \tag{80}$$

The current density of the superconductor coating by metal (fig.12) becomes

$$j^{(1)} = \sigma^{(1)} E = \left(x\sigma_s^{(1)} + (1-x)\sigma_m^{(1)}\right) E \tag{81}$$

In the model n is no longer expected to be independent of electric field and constant. Assume $j^{(1)} = j_c$ and the total current density is defined as

$$j = \sigma^{(1)} E \tag{82}$$

Using equation (79) and (77) where n is well defined, this leads to a new parameter $n(E)$ as function of the electric field (see Appendix E),

$$n = \frac{\sigma^{(1)}}{\sigma} = s\frac{x\sigma_s^{(1)} + (1-x)\sigma_m^{(1)}}{x\sigma_s^{(1)} + s(1-x)\sigma_m^{(1)}} = s\frac{x\sigma_s^{(1)} + \sigma_m^{(1)}}{xs\sigma_s^{(1)} + s(1-x)\sigma_m^{(1)} + (1-s)x\sigma_s^{(1)}} \tag{83}$$

One notices in (79) that $x\sigma_s^{(1)} + \sigma_m^{(1)} = \frac{j}{E}$ such that n can be written as dependent of electric field:

$$n(E) = s\frac{j}{j - (1-s)(1-x)\sigma_m E} \tag{84}$$

In thesis, I work with parameter τ in stead of electric field E. Also, n in(83)can be written as function of parameter τ. Parameter τ here is the sum of ratio in superconducting state and in ohmic state (for metal part),

$$\tau = \tau_s + \tau_m \tag{85}$$

The parameter τ for superconductor is $\tau_s = \frac{\kappa\mu_0 x\sigma_s}{SC}$ and the electric conductivity in superconductor is $\sigma_s = \frac{\tau_s sC}{x\mu_0\kappa}$. Same for metal, the parameter τ is $\tau_m = \frac{\kappa\mu_0(1-x)\sigma_m}{C}$ such that the electric conductivity in metal is $\sigma_m = \frac{\tau_m C}{(1-x)\mu_0\kappa}$. Insert all these parameters into (82), it gives n as function of τ,

$$n(\tau) = \frac{s\tau_s + \tau_m}{\tau_s + \tau_m} \tag{86}$$

The parameter τ_{total} is know from (84),(85) can be written in form:

$$n(\tau) = s - (s-1)\,\frac{\tau_m}{\tau} \tag{87}$$

This is important result because it makes easy to find the new dispersion equation for deposed metal case. In others words, insert (86) into equation (60), it gives (with assumption $\alpha = 1$ and $\frac{j}{j_c} = 1$):

$$\tilde{\lambda^2} + P\tilde{\lambda} + Q = 0 \tag{88}$$

where

$$P = \tilde{k}_x^2 + \frac{\tilde{k}_y^2}{n(\tau)} - \beta + \tau(\tilde{k}_x^2 + \tilde{k}_y^2) \tag{89}$$

$$Q = \tau\left(\tilde{k}_x^4 + \frac{n(\tau)+1}{n(\tau)}\tilde{k}_x^2\tilde{k}_y^2\right) + \frac{\beta}{n(\tau)}\left(\tilde{k}_x^2 - \tilde{k}_y^2\right) \tag{90}$$

The system is unstable if $\Re(\tilde{\lambda}(\tilde{k}_x, \tilde{k}_y)) > 0$

4.3 Result and Discussion

The model developed in previous subsection above led to dispersion equation for $\tilde{\lambda}$ in (87). The dispersion equation here takes in account the metal coating part and it determines when the system is unstable if $\Re(\tilde{\lambda}) > 0$.

Let start estimating the parameters τ and β for superconductors with metal coating geometry [see fig.12]. The calculations process is the same as in previous chapter. Here, the electric field must be calculated with the total electric conductivity $\sigma_{total} = \frac{x}{n}\sigma_s + (1-x)\sigma_m$ that includes the metal part.

Hereby the total electric field is $E = \frac{j_c}{n\sigma_{total}}$ such that

$$\tau_{max} = \frac{\kappa\mu_0 j_c}{nCE_{min}} \approx 3.7.10^{10} \tag{91}$$

and

$$\tau_{min} = \frac{\kappa\mu_0 j_c}{nCE_{max}} \approx 0.02 \tag{92}$$

The minimum and maximum of parameters β and the wave numbers that characterise the scale of the perturbation along the y and x axes (k_y and k_x) are the same as in previous chapter, namely $\beta_{min} = 0.02$,$\beta_{max} = 4.8$ and min $k_{x,y} = 0.02$ and max $k_{x,y} = 2\pi$ for $l = b$ and $l = 1mm$,respectively.

The results will be presented in 4 main parts (or subsubsections): a. phase diagram for flux jumps instability without metal coating, b. stability with deposed metal, c. the role of metals proprieties and d. the role of thickness.
Finally all important results will be concluded in subsection 'summary'.

4.3.1 Phase diagram for flux jumps instability without metal coating

In chapter 3, several plots and contour plots were made to study the instability in system without metal coating[fig.9,10 and 11].Those plots were analysed locally,i.e, they showed the instability for specific values of wave numbers k_x and k_y. Also, it does not represent the whole process in the system. To avoid this lack, Rakhmanov and co-authors in [1] already proposed a "hand" drawn phase diagram that predicts the whole instabilities in the system: stability's region, uniform jumps and fingering. I want to check out quantitatively this prediction/phase diagram. The result is in agreement with Rakhmanovs paper [1]. Let first consider the spatially uniform case where there exist a well-known criterion for thermo-magnetic instability[6]. With $k_y = 0$ and for very slow thermal diffusion,$\tau << 1$, the system is unstable if $k_x < 1$ according to equation(63). For Bean model, where $l = \frac{H}{j_c}$, this is expressed as

$$H > H_{adiab} = \frac{\pi}{2}\sqrt{\frac{CT_c}{\mu_0}} \tag{93}$$

In Rakhmanov paper[1],λ_{max}(see list of parameters,page 49) for k_x and k_y are calculated,

$$k_x^* = \frac{1}{\sqrt{n\tau}} \tag{94}$$

and

$$k_y^* = \left(\frac{2}{n}\right)^{\frac{1}{4}} \frac{1}{\sqrt{\tau}} \tag{95}$$

such that one can establish the threshold criterion for uniform and fingering,

$$E > E_c^{unif} = \frac{\pi^2}{4}\left(\frac{kT}{j_c l^2}\right) \tag{96}$$

and

$$E > E_c^{fing} = \frac{\mu_0 \kappa j_c}{C} \tag{97}$$

In thesis, I work with parameters τ and β. Parameter β is proportional to inverse wave number k_x that indicates the penetration depth of flux in superconductor. Using Bean model,the magnetic filed $H = j_c l$ where $l = \frac{\pi}{2k_x}$,and it gives

$$\frac{1}{k_x} = \frac{2H}{j_c \pi} \tag{98}$$

Finger instability can be obtained by using the heat capacity from (97) and (93). For $E > E_c$, it gives

$$H_{fing} = \frac{\pi}{2}\sqrt{\frac{CT_c j_c}{E}}, \tag{99}$$

One observes that there is a good agreement between analytical lines (96), (97), (99) and numerical calculation [see fig.13].

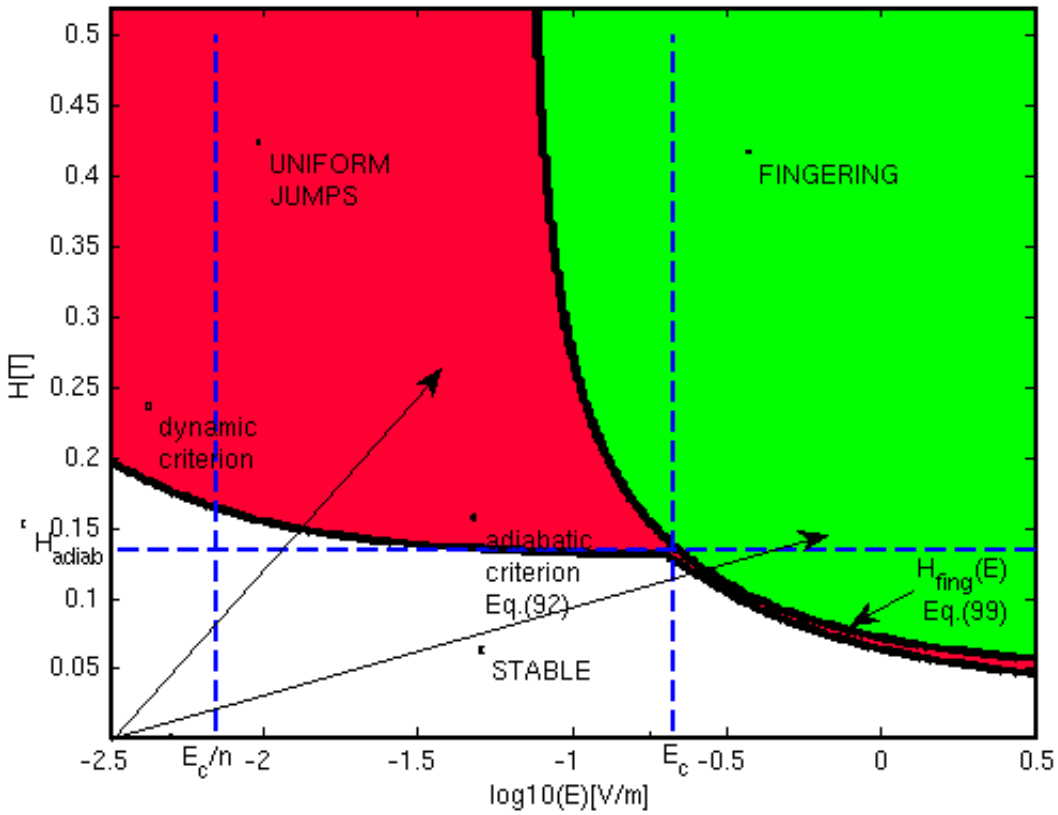

Figur 13: *Instability phase diagram in the plane magnetic field-electric field. The horizontal line corresponds to the adiabatic criterion for uniform jumps,Eq.(93).For $E > E_c$, the instability has a finger structure, and the criterion is given by Eq.(99)*

4.3.2 Stabilization of thermo-magnetic instability with metal coating

In previous chapter, the dispersion equation for $\tilde{\lambda}$ determines whether the system is unstable on criterion if $\Re(\tilde{\lambda}) > 0$. This is supported by plots and contours plots where the characteristic high and low electric field, and temperature dependent have been well showed[see fig.9,10 and 11]. On the other hand, alternative mechanism to stabilize the system have also been suggested, namely the metal coating.

To clarify this issue, the model built early in this chapter is a way to carry out a numerical solution to thermal and Maxwell equation.Let start with high and low electric field cases,i,e, with small and large parameter τ. Small τ means that the the instability increment $\Re(\tilde{\lambda})$ from (88)provides two mechanisms: a. slow heat diffusion where there is superconductor-Metal contact such that $\Re(\tilde{\lambda})$ is at finite k_y, b. the eletro-dynamic braking uses an electromagnetic force to suppress the fingers nucleating where there is not SC-Metal contact.

The suppression of the avalanches by providing a good thermal contact strongly suggests that the avalanches growth is associated with local heating. This is valid for uniform instability process with these two mechanisms above. Figure(14) reproduces figure(9) from chapter 3 and shows that the system becomes more stable when τ_m has a finite value different from zero.

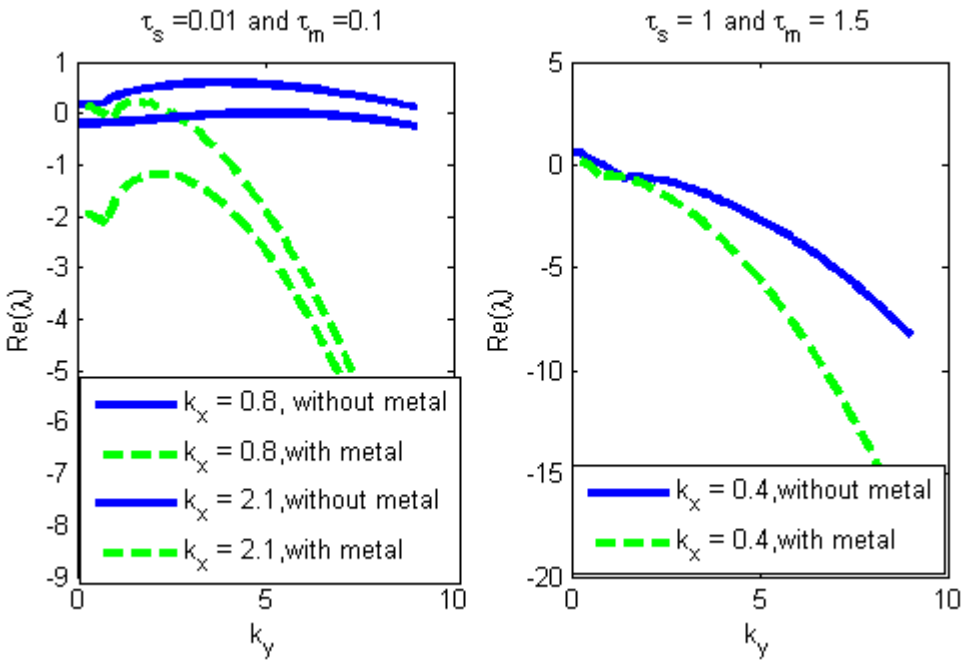

Figur 14: *The instability increment* $Re\lambda(k_y) found from Eq.(88). Both cases, with/without metal coating for$: *a.small* τ_s*,high electric field, b. for large* τ_s*, low electric field. Both plots show that the system becomes more stable when* $\tau_m \neq 0$*,i.e,metal contribution.*

In figure 14 parameter β is fixed,$\beta = 1$. This means that the system is temperature independent from external source. Let draw a contour plot of $\tilde{\lambda}_{max}$ as function of τ and β. And the penetration depth

$$l = \frac{2\pi}{k_x} \tag{100}$$

Figure 15 shows that the system was initial unstable in region between [1.28,1.6]. This region is stabilized with metal coating. In addition, figure 15 shows that $k_{x,y}$ ensure the system to become more stable with increasing of their values. This is expected since $k_{x,y}$ is related to flux penetration

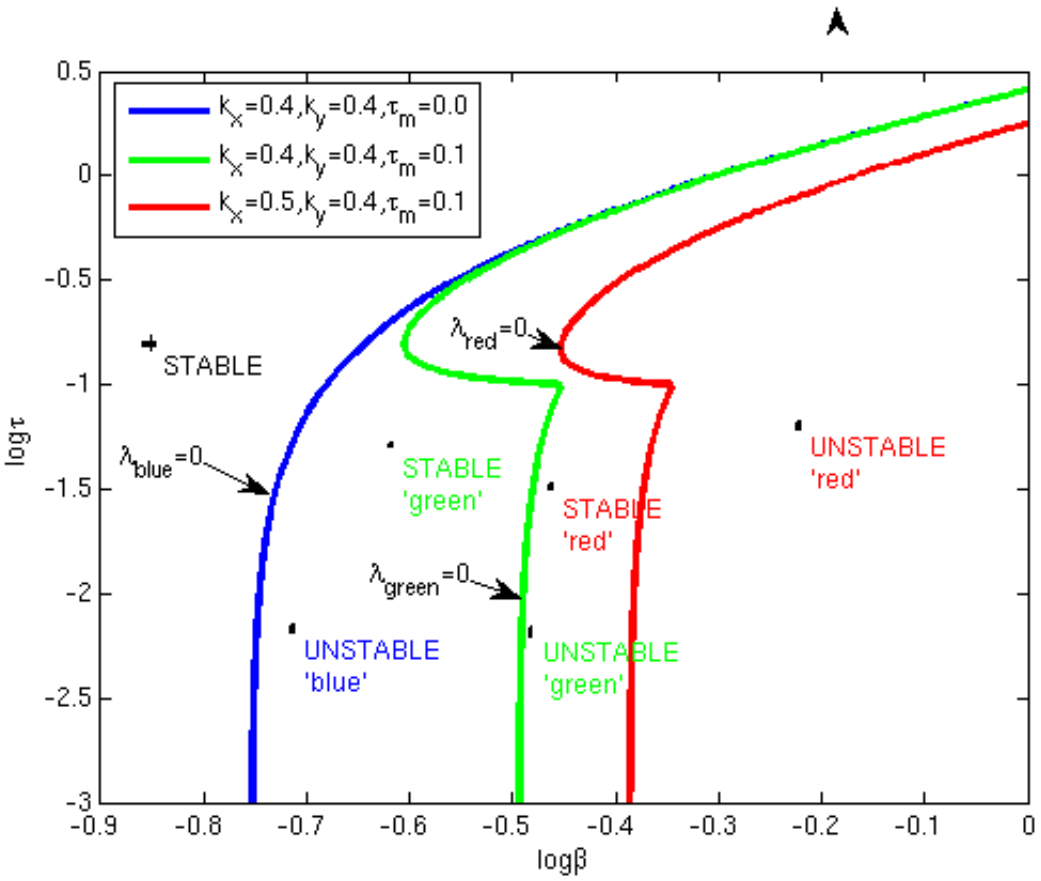

Figur 15: *This is zero contour plot of max* $\Re(\lambda)$ *from Eq.(88) as function of parameters* τ *and* β. *The blue line is the case with no metal coating*($\tau_m = 0$), *the green and the red line is the case with metal coating*($\tau_m = 0.1$).$s = 10$ *in Equ.(87). One sees the deposed metal makes the system to be more stable,i.e, it increases the stability region.In addition red line shows that the system becomes more stable when* k_x, *the wave number that characterises the flux penetration,increases.*

depth. The lack to the contour plot and the plot in figure 14 and 15 is that the values of $k_{x,y}$ are fixed. This means that the stabilization is studied locally and it limits our knowledge for the rest of system. I mentioned early that the phase diagram solves this problem [see fig.13]. It represent the entire system with electric field and magnetic field in x and y-axes,respectively.Figure 16 shows this later statement,i.e, the region where stability in system occurs for all k_x and k_y.[see fig.16]

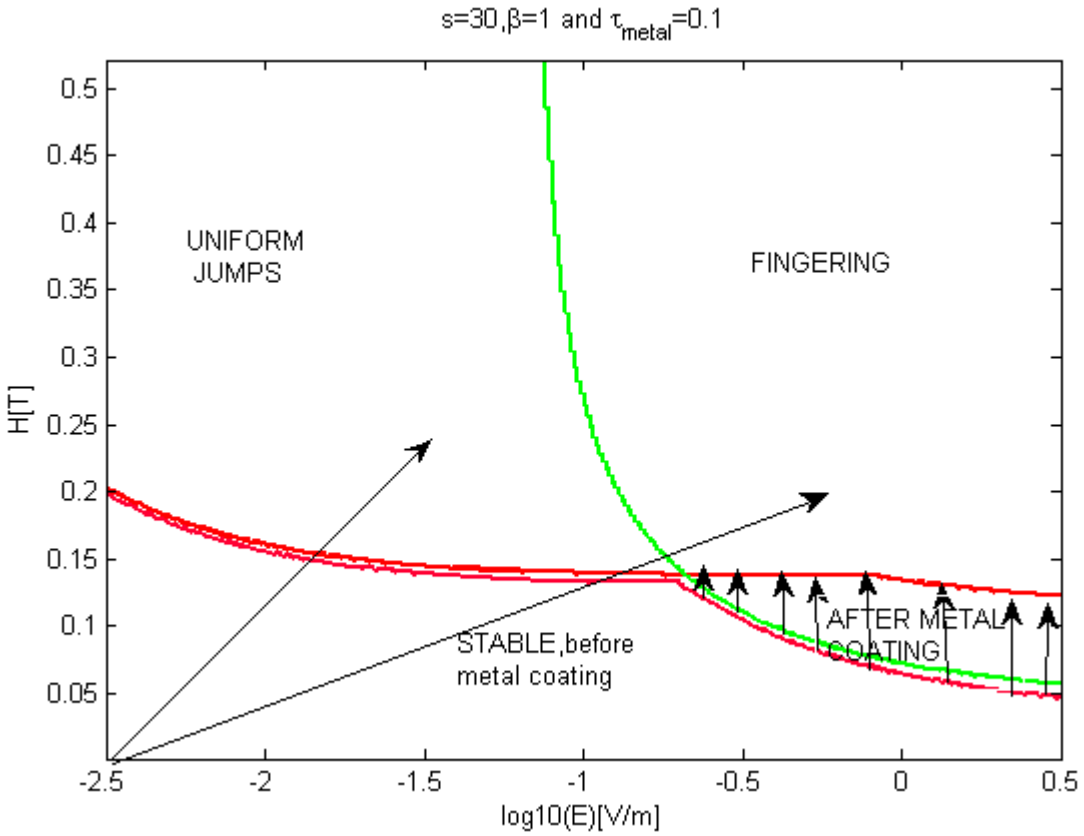

Figur 16: *This is the instability phase diagram in the plane magnetic field-electric field.Stability's area increases after been coated with metal.This shows that the metal suppressed the sudden appearance of the fingering flux avalanches.*

Numerical estimates in figure 16 were made using parameters for low-temperature superconductors at helium temperatures: $j_c = 10^{10}A/m^2$, $C = 10^3 J/Km^3$, $T_c = 39K$,and $n = 30$. Figure 16 shows that the uniform instability development is preferable for low electric fields, more exactly for $E < E_c/n$ [see fig.15]. One observe from figure 16 that the finger instability occurs only at rather large background electric field ($\approx 0.18V/m$,bear in mind that is log10(E)in x-axe). I mean, let increase the magnetic field with a rate of H by starting moving along a straight line form the origin.

For large $\dot{H}$, the stability is destroyed for smaller H, and resulting in formation of a nonuniform spatial structure. Metal coating suppress this nucleation ,i.e, increases the stability's area as i mentioned early. This can be considered as covered part in superconductor. One observes that no finger patterns are seen to be nucleating in the covered part. Even fingers that nucleated in the uncovered part of the superconductor do not propagate into the adjacent covered part [2].

4.3.3 Role of metal proprieties in stabilisation process

It is clear above that the metal coating affects the thermomagnetic instability in superconductors. In my numeric calculation and analytic, it means that the value of parameter τ is different from zero or larger than zero. It is experimentally confirmed that the metal deposition does no adversely affect the superconducting properties. In others words, the presence of metal has no other consequence for the current carrying capacity of the superconductors than to suppress the instability.

The $\Re(\tilde{\lambda})$ in (88) decreases dramatically when parameter τ_m, the ratio between thermal and magnetic diffusion in metal, increases. It means that the conductivity of metal has a crucial role in stabilisation of thermomagnetic instability in superconductors. Metal with high thermal conductivity κ correspond to thermal contact as reason for suppression of avalanches, and with high electric conductivity corresponds to electrodynamic braking as reason for suppression of avalanches. Figure 17.a shows phase diagrams with two different metals($\rho = 1.310^{-9}\Omega m$,$\rho = 1.310^{-10}\Omega m$). In figure 17.b, both metals are compared with superconductor without metal coating ($\tau_m = 0$). This shows that the system is more stabilized for metal with low resistivity($\rho = 1.310^{-10}\Omega m$) than the another one with resistivity $\rho = 1.310^{-9}\Omega m$. This is an expected result and it can simply be explained with equations in section 4.2 (on pages 30-32). I am talking about the conductivity of metal σ_m. It is known that the conductivity is defined as inverse resistivity ρ. It has been seen in section(4.2) that the ratio between the thermal and magnetic diffusion τ_m in metal is proportional to the conductivity ,

$$\sigma_m = \frac{\tau_m C}{\kappa \mu_0 (1-x)} \tag{101}$$

where $(1-x)$ is the non-superconducting parts(see fig.12).

Larger conductivity in metal corresponds to larger ratio τ_m and meaning larger τ_{total} since it is the sum of superconducting and metallic parts. It was shown in chapter 3 that the system has uniform mode for large parameter τ such that it becomes more stable if τ keeps increasing. Here the importance of thermal stabilization between superconductor-metal is necessary to explain thermomagnetic instability. Using numeric estimations above, the electric conductivity σ_m gives,

$$\sigma_m = \frac{10^{12}}{4\pi}\tau_m = 10^{11}\tau_m \tag{102}$$

such that the electric field gives,

$$E = \frac{j_c}{\sigma_m} = 10^{-1}\frac{1}{\sigma_m} \tag{103}$$

The instability occurs essentially when $\tau_s \simeq \tau_m$,where $\sigma_m = \frac{j_c}{SE}$ in superconductor. The electric field now is

$$E = 10^{-1}\frac{1}{S\tau_m} \tag{104}$$

Estimations for electric fields with resistivity $\rho_m = 10^{-9}\Omega m$ is $E \simeq 0.3V/m(log10(E) \simeq -0.53V/m$ in fig.17) and with resistivity $\rho_m = 10^{-10}\Omega m$ is $E \simeq 0.03V/m$. Thus, the stabilisation of the system depends on proprieties of metal. A metal with high conductivities will stabilize the superconductors better than metal with poor conductivity.

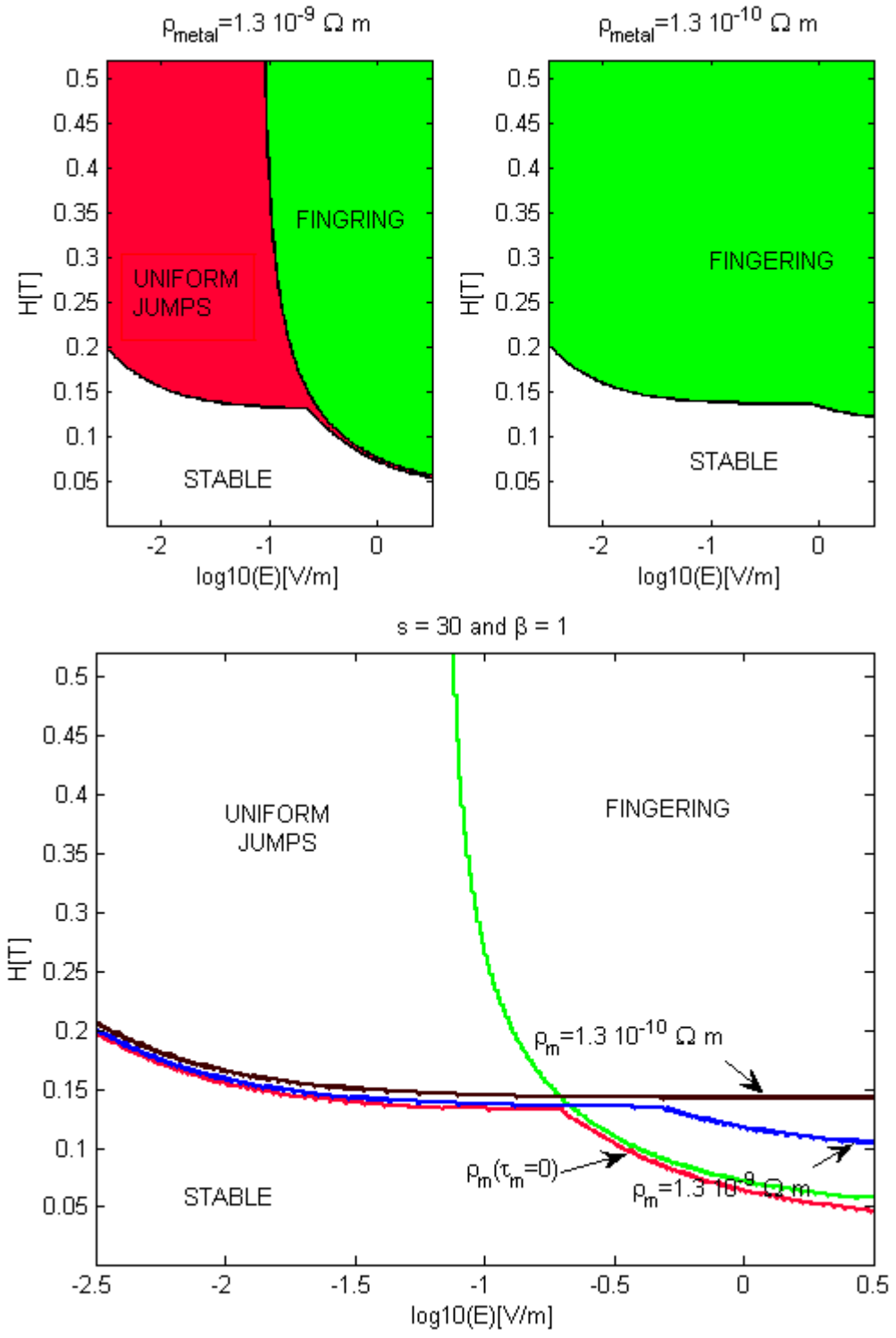

Figur 17: *This is the instability phase diagram in the plane magnetic-electric field showing the stabilisation with two different metals: a. metal A (with* $\rho = 10^{-9}\Omega m$*) and metal B (with* $\rho = 10^{-10}\Omega m$*). b. the stabilisation area for metal B is larger than the one for metal A.This means that metal with low resistivity or high conductivity stabilizes the system better than poor metal with high resistivity or low conductivity.*

4.3.4 The role of thickness in stabilisation process

Until now i started with assumption that I choose a specific value of x for equations above. All plots and contour plot were drawn on this assumption. the parameter x is the fraction of superconducting part and $(1-x)$ is the fraction of non-superconducting part "metal". Figure 18 shows the suppression of avalanches or the stabilisation of the system has a gradual tendency, directly related to the decrease of the metal-superconductor spacing. The physical interpretation is that the braking will by Faraday induction low act in opposition to the rapid temporal variation in the flux. This means that the system becomes more stable when x decreases. Group of professor Choi showed this statement with experiment[see fig.2 in chapter 1].

To make a contour plot showing the effect of thickness on stability, I had to include x in my Matlab code. The simple way to do it was like this: Parameter β depends on critical density j_c and j_c has superconducting fraction x (see Appendix E). Using equation (53) in chapter 2, it makes parameter β to be proportional to x^2 such that

$$\beta = x^2\beta_0 \tag{105}$$

Similar for anther parameters contains x

$$\tau_m = (1-x)\tau_{m0} \tag{106}$$

$$\tau_s = x\tau_{s0} \tag{107}$$

and

$$r = \frac{j}{j_c} = 1 + \frac{1}{s}\frac{(1-x)\tau_{m0}}{x\tau_{s0}} \tag{108}$$

where τ_{m0}, τ_{s0} and β_0 are constant.

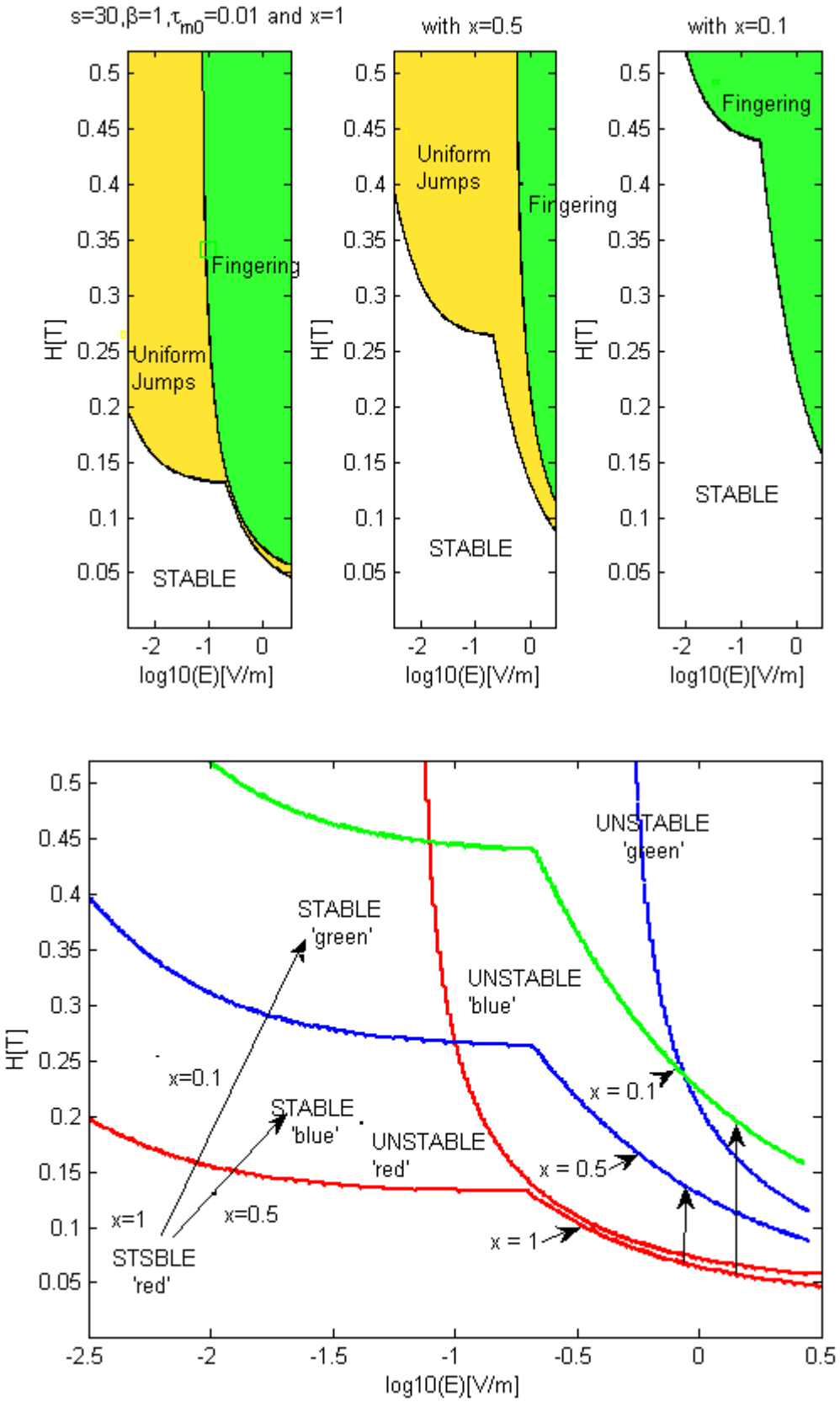

Figur 18: *This is the stability phase diagram in the plane magnetic-electric field showing the stabilisation of the system with covered metal (With* τ_{s0}= 0.1 *and* $\tau_{m0} = 0.01$,*see Eq.106-107) thickness of: a)*$a = 1$, *b)*$x = 0.5$, *c)*$x = 0.1$.*In fig.18 B all three phase diagrams are represented together. The diagrams show that the system becomes more stable with decreasing* x.*Parameter* τ_m*(or* σ_m*) increases as consequence of decreasing* x. *Higher conductivity* σ_m *stabilized the system as showed in fig.17 above.*

4.4 Summary

The suppression of avalanches with metal coating is studied in chapter 4. This effect or suppression is due to the electromagnetic braking that takes place during the deposing of metal. The metal does not need to be in contact with the superconductor and has no other consequence for the carrying capacity of superconductor.

Electrodynamic braking effect is suggested to be responsible for suppression of finger in superconductors. One might consider this effect as a complementary of thermal contact described in previous chapter. By using a simple model built to support the electrodynamic brake, it led to a dispersion equation for $\tilde{\lambda}$. This quadratic equation determines the instability of the system.

Plots and contour were made from it to show the stability dependency on metal proprieties, on thickness and to confirm the fact that metal coating indeed suppress the thermo-magnetic instability in superconductor. Another observation is the dependency on k_x. The wave number k_x characterises the perturbation scale in superconductor.It is obvious that the system becomes more stable for corresponding larger k_x since this wave number is proportional to flux jumps penetration length.

.

Chapter 5

5 Onset/Offset of oscillations

This chapter can be considered as an extra part of thesis. It is about the study of oscillations that might be observed under certain conditions. I found interesting to take a quick look on it. There are not many papers treating the case of imaginary solution even if it has no really scientific interest. Early in thesis, solutions to dispersion equation for $\tilde{\lambda}$ were found as:

$$\tilde{\lambda}_1 = \frac{-P + \sqrt{P^2 - 4Q}}{2} \tag{109}$$

and

$$\tilde{\lambda}_2 = \frac{-P - \sqrt{P^2 - 4Q}}{2} \tag{110}$$

where

$$P = \tilde{k}_x^2 + \frac{\tilde{k}_y^2}{n(\tau)} - \beta + \tau(\tilde{k}_x^2 + \tilde{k}_y^2) \tag{111}$$

$$Q = \tau\left(\tilde{k}_x^4 + \frac{n(\tau)(\tau)+1}{n(\tau)}\tilde{k}_x^2\tilde{k}_y^2\right) + \frac{\beta}{n(\tau)}\left(\tilde{k}_x^2 - \tilde{k}_y^2\right) \tag{112}$$

Following Table.2 (page 56), one expects to observe oscillations when $P^2 < 4Q$. Let start with mathematical analysis of this system such that it gives an overview and finally a physical interpretation can be suggested. It is clear that solutions in (109) and (110) belong to imaginary part if the condition above is satisfied. It implies that

$$Q > \frac{P^2}{4} \in \Re \tag{113}$$

There are two possibilities in (113), $P = 0$ and $P \neq 0$. Let us focus on the first one:

$P = 0$ means that $Q > 0$ and (101) gives

$$\tilde{\lambda} = \pm\sqrt{-Q} \tag{114}$$

These are complex solutions since $Q > 0$ and $Q < 0$ does not fulfil the main condition, namely $P^2 < 4Q$. But $Q = 0$ gives one solution $\lambda = 0$. Insert Q with condition $Q > 0$ into (95) and one find the condition for onset of oscillation when $P = 0$:

$$\tau > \frac{\beta\left(\tilde{k}_y^2 - \tilde{k}_x^2\right)}{\left(n\tilde{k}_x^4 + (n+1)\tilde{k}_x^2\tilde{k}_y^2 + \tilde{k}_y^4\right)} \tag{115}$$

For metal case, it is similar but it is best to find the condition with parameter β in stead of τ since parameter n is function of τ. Also, it gives

$$\beta > \frac{\tau\left(\tilde{k}_x^4 + \frac{n(\tau)+1}{n(\tau)}\tilde{k}_x\tilde{k}_y + \frac{\tilde{k}_y^4}{n(\tau)}\right)}{\tilde{k}_y^2 - \tilde{k}_x^2} \tag{116}$$

where $n(\tau) = s - (s-1)\frac{\tau_m}{\tau}$ For both cases,with and without deposed metal, the observations are equivalent since $n(\tau)$ does not change much the imaginary solutions.

The physical interpretation concerning the onset/offset of oscillations is that the oscillations appear when one attains the borders zone between stable and unstable regions. The system has tendency to go up to "unstable state", then goes down to " stable state". This up-down motion is called thermo-magnetic oscillations.

.

Chapter 6

6 Main conclusions

The idea to suppress the avalanches with metal is old; several theoretical and experimental frameworks have been established to describe this phenomenon[2],[3],[4],[9]. Superconducting cables are embedded in metal such that the suppression of flux jumps takes place in superconductors. It can be due to the improved heat conductivity in the metal layer. Recently, Fabianos experiment [49] showed that the metal does not need to be in contact with superconducting sample to observe suppression of thermomagnetic instability in superconductor. It means that the thermal contact is not the only reason for stabilization of thermomagnetic instability, but the electrodynamic braking might be responsible for this effect.

In thesis, I essentially apply the known idea about the thermo-magnetic instability to electrodynamic braking. The electrodynamic braking is suggested to describe the suppression of avalanches in superconductor with metal in sandwich form geometry[see fig.12]. This effect stops or suppresses the motion of flux jumps in superconducting sample using electromagnetic force. My work focused on this breaking effect. A model for electrodynamic braking was made to explain the suppression of exciting type of avalanches and to prove that the early experiments [2] and [3] work theoretically.

To study the thermomagnetic instability that takes place in superconductor, the linear stability analysis of thermal diffusion and simple electrodynamic equations of Maxwell seems to be useful. I analyzed the thermomagnetic instability in superconductor by starting to establish the boundary condition and solving the quadratic equation. The suppression of thermomagnetic instability due to thermal contact is briefly treated in chapter 3 since there are many publications that confirm theoretically and experimentally this case.

For electrodynamic braking theory, a simple model based on Gurevich and Mints paper [3] was built. The model consists of a superconducting sample coating by a metal layer in sandwich form. The model leads to a dispersion equation for instability increment. Solving this quadratic or dispersion equation, it gives physical interpretation of stability in steak of superconductors and metal, and the results are:

a. Factor $n(\tau)$ in (86) decreases when the conductivity for metal is added. Decreasing $n(\tau)$ corresponds to large stability in superconductors since the maximal real part of dispersion equation for instability increment becomes negative. Also, the system becomes more stable against nucleation.[see fig.14 , fig.15 fig.16]

b. Increasing values of the wave number $\tilde{k}_x$ ensure that the system becomes more stable. This is related to the fact that large values of $\tilde{k_x}$ corresponds to small depth of flux penetration, and hence to more stable situation.[see fig.15]

c. Larger conductivity of metal leads to large stability in superconducting sample. The conductivity of metal σ_m corresponds to small parameter in equation (54) such that the system becomes more stable [see fig.17]. The result in this figure 17 is a prediction that can be tested on a new experiment.

d. Increasing the thickness of metal layer leads to stabilize the superconducting sample efficiently. This is based on equation (87) taking in account the metallic part through ratio between the current density j and critical current density j_c(see Appendix F). The result is in agreement with experimental results[5].[see fig.18]

.

List of parameters

- j: current density.
- j_c: critical current density.
- b: The length scale.
- C: specific heat capacity.
- T: temperature.
- T_c: critical temperature.
- τ: dimensionless parameter, ratio between thermal and magnetic diffusion
- τ_m: ratio between thermal and magnetic diffusion in metal.
- τ_s: ratio between thermal and magnetic diffusion in superconductor.
- β: dimensionless parameter that characterize the perturbation form external source.
- t_0: the time scale.
- λ: dimensionless parameter(see Equ.60).
- $\tilde{\lambda}$: $\tilde{\lambda} = t_0\lambda$.
- $\tilde{\lambda}_{max}$: maximum real solutions of dispersion equation for $\tilde{\lambda}$ and determine whenever the system is unstable.
- λ_L: London penetration depth
- ξ: coherence length
- κ: a) thermal conductivity, b) Ginzburg-Landau parameter,ratio between London penetration depth and coherence length.
- ρ: resistivity.
- ρ_0: initial resistivity.
- k_x and k_y: wave numbers that characterizes the scale for perturbation.
- $\tilde{k_x}$ and $\tilde{k_y}$: $\tilde{k_{x,y}} = bk_{x,y}$
- σ: differential electric conductivity defined as $\sigma = \frac{\partial j}{\partial E}$.
- x: the fraction of superconducting part (see fig.12)
- $\sigma_s^{(1)}$: electric conductivity in superconductor.
- σ_s: differential conductivity in superconductor.
- σ_m: electric conductivity in metal.
- s: ratio between the electric conductivity and differential conductivity
- $\sigma^{(1)}$: total electric conductivity of superconductor coated with metal
- $j_s^{(1)}$: current density in superconductor
- α: dimensionless parameter, defined as the product between the resistivity and the electric conductivity.

Figurer

.

Appendix

A. Proof of $\delta E = \delta E_y$ and $\delta j = \delta j_y$,assume $E_x = 0$ and $j_x = 0$

$E + \delta E = \sqrt{(E_x + \delta E_x)^2 + (E_y + \delta E)^2}$
$= \sqrt{E_x^2 + 2E_x\delta E_x + E_x + 2E_y\delta E_y + E_y^2}$
$= \left(E^2 + 2E_y\right)^{1/2} = E + \delta E_y$

$$E + \delta E = E + \delta E_y \tag{117}$$

Similar process for the current density, $j + \delta j = \sqrt{(j_x + \delta j_x)^2 + (j_y + \delta j)^2}$
$= \sqrt{j_x^2 + 2j_x\delta j_x + j_x + 2j_y\delta j_y + j_y^2}$
$= \left(j^2 + 2j\delta j_y\right)^{1/2}$

$$j + \delta j = j + \delta j_y \tag{118}$$

B. Proof of the current voltage curve

The exact form of current voltage curve can be written in this form,

$$\overrightarrow{j} = j\left(T, E\right)\left(\frac{\overrightarrow{E}}{E}\right) \tag{119}$$

Since the vector $\overrightarrow{E}$ is parallel to the $y$axis, it has been showed in appendix A $\delta E = \delta E_y$. As result of linearisation of current-voltage curve, one can show that

$$\delta\overrightarrow{j} = \left(\frac{\partial j_c}{\partial T}\delta T + \sigma\delta E_y\right)\frac{\overrightarrow{E}}{E + j_c\frac{\delta E_x}{E}} \tag{120}$$

also,

$$\overrightarrow{j} + \delta\overrightarrow{j} = \overrightarrow{j}(E, T) + \frac{\partial\overrightarrow{j}}{\partial E_x}_x + \frac{\partial\overrightarrow{j}}{\partial E_y}_y + \frac{\partial\overrightarrow{j}}{\partial T}\delta T \tag{121}$$

Reduce (121) with definition in (119) and it gives,

$$\delta\overrightarrow{j} = \frac{\partial\overrightarrow{j}}{\partial E_x}\delta E_x + \frac{\partial\overrightarrow{j}}{\partial E_y}\delta E_y + \frac{\partial\overrightarrow{j}}{\partial T}\delta T \tag{122}$$

Insert the differential conductivity $\sigma = \frac{\partial\overrightarrow{j}}{\partial E_y}$ in (122) and assume $\overrightarrow{j} = j_c$ in x-axis, it gives

$$\delta\overrightarrow{j} = \frac{\partial\overrightarrow{j_x}}{\partial E_x}\delta E_x + \sigma\delta E_y + \frac{\partial j_c}{\partial T}\delta T \tag{123}$$

Thus the linearisation of (123) can finally be shown,

$$\overrightarrow{j}\left(\overrightarrow{E} + \delta\overrightarrow{E}, T + \delta T\right)\frac{\overrightarrow{E}}{E} = \left(\overrightarrow{j} + \delta\overrightarrow{j}\right)\frac{\overrightarrow{E}}{E} \tag{124}$$

$$\delta\overrightarrow{j} = \left(\frac{\partial j_c}{\partial T} + \sigma_y\right)\frac{\overrightarrow{E}}{E} + j_c\frac{\delta E_x}{E} \tag{125}$$

C. The electric conductivity in SC σ_s

The total current density is defined as

$$\overrightarrow{j} = \sigma_s \overrightarrow{E} \tag{126}$$

where the total electric conductivity $\sigma_{total} = x\sigma_s + (1-x)$ and x is the factor of superconducting part. By choosing $x = 1$, it gives

$$\overrightarrow{j} = \sigma_s \overrightarrow{E} \tag{127}$$

The electric conductivity in superconductor can be found now. One often uses the power law relation:

$$E = \rho_0 \left(\frac{j}{j_c}\right)^n j_c \tag{128}$$

Let find the fraction $\left(\frac{j}{j_c}\right)^n = \frac{E}{\rho_0 j_c}$,

$$\frac{j}{j_c} = \left(\frac{E}{\rho j_c}\right)^{\frac{1}{n}} \tag{129}$$

Insert (129) into (128), it gives

$$E = \rho \left(\frac{E}{\rho_0 j_c}\right)^{\frac{n-1}{n}} \overrightarrow{j} \tag{130}$$

Such that $\overrightarrow{j} = \frac{1}{\rho_0}\left(\frac{E}{\rho_0 j_c}\right)^{\frac{n-1}{n}} \overrightarrow{E} = \sigma_s \overrightarrow{E}$. Also, the electric conductivity in superconductor is

$$\sigma_s = \sigma_0 \left(\frac{E}{E_0}\right)^{\frac{n-1}{n}} \tag{131}$$

D. Relationship between differential conductivity σ and conductivity in SC σ_s

In appendix C above, the current density was found to be

$$j = \sigma_0 \left(\frac{E}{E_0}\right)^{\frac{n-1}{n}} \overrightarrow{E} = \frac{\sigma_0}{E_0^{-1}} \left(\frac{E}{E_0}\right)^{\frac{1}{n}} \tag{132}$$

The differential conductivity is $\sigma = \frac{\partial j}{\partial E}$ such that it gives

$$\sigma = \frac{\partial j}{\partial E} = \frac{1}{n}\sigma_0 \left(\frac{E}{E_0}\right)^{\frac{n-1}{n}} \tag{133}$$

$$\sigma = \frac{1}{n}\sigma_s \tag{134}$$

Also, the relationship between differential conductivity and conductivity in SC without metal coating is

$$\sigma = \frac{1}{n}\sigma_s \tag{135}$$

E. n as function of parameter τ

The parameter n is defined as $n \equiv \frac{j_c}{\sigma E}$ and assuming Mints and Gurevichs model in [3], the total conductivity is $\sigma^{(1)} = \sigma_{total} = x\sigma_s + (1-x)\,\sigma_m$. Using (), it gives

$$E = \frac{j}{x\sigma_s + (1-x)\sigma_m} \tag{136}$$

Insert (136) into $n \equiv \frac{j_c}{\sigma E}$, it gives

$$n = s\frac{x\sigma_s + (1-x)\sigma_m}{x\sigma_s + s(1-x)\sigma_m} \tag{137}$$

Where the electric conductivity in metal is $\sigma_m = \frac{\tau_m C}{\mu_0 \kappa (1-x)}$

Insert the rest of parameters into (137) , n can be written in another form as function of electric field ,

$$n(E) = s\frac{j}{j - (1-s)(1-x)\sigma_m E} \tag{138}$$

Or as a function of parameter τ,

$$n(\tau) = s - (s-1)\,\frac{\tau_m}{\tau_{total}} \tag{139}$$

F. Dimensionless ratio $\frac{j}{j_c}$

Assume the superconductor geometry in sandwich form (see fig.12), the total current density is sum of metal and superconductor parts:

$$j = xj_s + (1-x)\sigma_m E \tag{140}$$

Where j_c is the current density in superconductor,x is the superconducting fraction part and $(1-x)$the non-superconducting part, and σ_m is the electric conductivity in metal.

Consider $j_s = j_c$ in superconductor such that the dimensionless ratio:

$$\frac{j}{j_c} = \frac{xj_c + (1-x)\sigma_m E}{xj_c} = 1 + \frac{(1-x)\sigma_m E}{xj_c} \tag{141}$$

Let call this ratio $r = \frac{j}{j_c}$ and r can be express with parameter τ terms. The parameter τ is the sum of superconducting and metal parts,

$$\tau = \tau_s + \tau_m \tag{142}$$

Where $\tau_s = \frac{x\mu_0\kappa\sigma_s}{C}$ and $\frac{(1-x)\mu_0\kappa\sigma_m}{C}$ The fraction between these two ratios σ_m and σ_s is

$$\frac{\tau_m}{\tau_s} = -\frac{x\sigma_m s E}{xj_s} \tag{143}$$

Insert (143) into (141), it gives

$$r = \frac{j}{j_c} = 1 + \frac{1}{s}\frac{\tau_m}{\tau_s} \tag{144}$$

.

Resistivity ρ	$7\mu\omega cm$
Thermal conductivity κ	170 W/Km$(\frac{T}{T_c})^3$
Heat Capacity C	$35kJ/Km^3(\frac{T}{T_c})^3$
Critical temperature T_c	39 K
Critical current at $T = 0K$	$10^{11}A/m^2$
Thickness d	400 nm
Strip half-width	2 mm
Temperature T_0	$0.15T_c$

Max $\Re(\tilde{\lambda}) < 0$	Max $\Re(\tilde{\lambda}) > 0$	$\tilde{\lambda} = \frac{-P+\sqrt{P^2-4Q}}{2}$
Stable; No oscillations	Unstable No oscillations	$P^2 > 4Q$, real solutions
Stable	Unstable	$P^2 < 4Q$, imaginary solution
Oscillations	Oscillations	$P^2 < 4Q$, imaginary solutions

Table.1 and 2 : 1. parameters values of MgB_2, 2. Solutions to dispersion equation for $\tilde{\lambda}$

.

Referanser

[1] A.L.Rakhmanov, D.V.Shantsev, Y.M.Galperin and T.H.Johansen: *Phys.Rev*, **B 70** ,224502 (2004)

[2] R.G.Mints, A.L.Rakhmanov: *Rev.Mod.Phys*, **53** ,551 (1981)

[3] A.V.Gurevich: *'Self heating'*, New York (1997)

[4] E.M.Choi, H.S.Lee, H.J.Kim and B.Kang: *App.Rev.*, Let.**87** ,152501(2005)

[5] D.V.Denisov, D.V.Shantsev, Y.M.Galperin, E.M.Choi, H.S.Lee, S.I.Lee, A.V.Bobyl,P.E.Goa,A.A.F.Olsen and T.H.Johansen: *Phys.Rev*, **Lett. 97** ,077002(2006)

[6] D.V.Denisov, D.V.Shantsev, Y.M.Galperin and T.H.JOhansen: *Phys.Rev*, **B 73**,014512(2006)

[7] V.V.Yurchenko, D.V.Shantsev, M.R.Nevala, I.J.Maasilta, K.Senapati, R.C.Budhani and T.H.Johansen: *Phys.Rev*, **B 90** ,224442 (2007)

[8] A.P.Sutton: *Oxford*,'Electronic Structure of Materials' **Oxford Science Publications**2004)

[9] Z.Fisk, H.R.Ott: *Elsevier*, 'Comtemporary Concepts of Condensed Matter Science' (2011)

[10] A.K.Saxena: *Springer*, 'High Temperature Superconductors', *Springer*(2010)

[11] D.J.Griffiths: 'Introduction to Quantum Mechanics' *Pearson,Second Edition*(2005)

[12] R.Tilley: *Willey Longman Edition* 'Understanding Solids'(2011)

[13] D.V.Schroeder: 'Thermal Physics' *Willey Longman Edition*(2000)

[14] M.Baziljevich, D.V.Shantsev, Y.M.Galperin, E.M.Choi, H.S.Lee, S.I.Lee, P.E.Goa and T.H.Johansen: *Europhys*, **Lett. 59** ,599(2002)

[15] G.Mints, A.L.Rakhmanov: *J.Phys*, **Appl.hys. 9** ,2281(1976)

[16] M.N.Wilson: 'Superconducting magnets', *Oxford ClarendonPress*(1983)

[17] B.Surzhenko, S.Schauroth, D.Litzkendorf, M.Zeisberger, T.Habisreuther and W.Gawalek: *Supercond.*, **Sci.Techno. 14** ,70(2001)

[18] R.G.Mints: *JETP.*, **Lett. 27** ,417(1978)

[19] Hancox: *Phys.Rev*, **Lett. 16** ,208(1965)

[20] U.Bolz, J.Schiessling, B.U.Runge, P.Leiderer: *Physica.*, **B. 284** ,288757(2000)

[21] C.P.Bean: *Phys.Rev.Lett.*, **B. 8** ,250(1962)

[22] C.P.Bean: *Mod.Phys.Rev*, **B. 36** ,31(1964)

[23] J.Albrecht and H.U.Habermeier: *Phys.Rev*, **Lett. 98** ,117(2007)

[24] D.V.Denisov: *et al.Phys.Rev*, **B. 73** ,014512(2006)

[25] M.Baziljevich: *et al.Phys.Rev. Amsterdam*, **C. 369** ,93(2002)

[26] M.Xu, D.Shi and F.Fox: *Phys. Rev.*, **B. 42** ,10773(1990)

[27] L.Ji, R.H.Sohn, G.C.Spalding,C.J.Lobb and M.Tinkham: *Phys. Rev.*, **B. 40** ,10936(1989)

[28] Y.B.KIM, C.F.Hempstead and A.R.Stranad: *Phys. Rev.*, **B. 9** ,306-309(1989)

[29] L.Legrand, I.Rosenman, C.Simon and G.Collin: *Physica*, **C. 211** ,239(1993)

[30] K.Eliasen: Master thesis, *'Investigation of thermomagnetic instability in superconducting NbN thin-films by automated real-time magneto-optical imaging'*(2007)

[31] A.Abrikosov: *Soviet Physics JETP 5.*, **B. 1442** ,1452(1957)

[32] H.Kamerlingh Onnes: *Leiden Communications*, 12 ,120(1911)

[33] F.Kedves: *Estimation of maximum electrical resistivity of High Critical Temperature*, Solid State Communications ,63:991-992(1987)

[34] C.Poole, H.Farach, R.Creswick and R.Prozorov: *Academic Press*, Second Edition(2007)

[35] "CERN releases analysis of LHC incident"(Press release). CERN Press Office. 16 October 2008. Retrieved 2009-09-28.

[36] "CERN inaugurates the LHC"(Press release). CERN Press Office. 21 October 2008. Retrieved 2008-10-21.

[37] E.Altshuler and T.H.Johansen: *Phys.Rev.Mod.*,0034-6861 Volume ,**76**(2004)

[38] A.Abrikosov: *Soviet Physics JETP 5.*, **B. 1442** ,1452(1957)

[39] V.K.Christensen,V.Malthe-SÃ¸rensen,J.Feder,T.JÃ¸ssang and P.Meakin: *Nature.London* **379** ,49(1996)

[40] R.R.Cruz and E.Altshuler: *Phys.Rev.*, **B. 63** ,094501(2001)

[41] C.J.C.Reichhardt and F.Nori: *Phys.Rev.*, **B. 56** ,6175(1997)

[42] de Gennes,P.G: *Superconductivity of Metals and Alloys*, (Benjamin ,New York)((1966)

[43] R.J.Zieve, J.R.Clem, M.McElfresh, and M.Darwin: *Phys.Rev*, **(B 49)**9802((1966)

[44] G.Blatter, M.V.Feigel'man, A.I.Larkin, and V.M.Vinokur: *Mod.Rev*, **(66)**, 9802((1994)

[45] C.A Duran: *Phys.Rev*, **B 52)**, 751195((1995)

[46] P.Leideren: *et al.Phys.Rev*, **Lett. 71)**, 751195((1993)

[47] S.Jin, H.Mavoori, C.Bower: *Nature*, 411, 563-565(2001)

[48] I.Aranson, A.Gurevich, M.Welling, R.Wijngaarden, V.Vlasko-Vlasov, V.Vinokur, and U.Welp: *Phys.Rev.Lett.*, **B 94)**, 037002((2005)

[49] C.Fabiano, E.Choi, J.Lee, S.I.Lee, E.J.Patino, M.G.Blamire, and T.H.Johansen: *et al. App.Phys.Rev.*, ISSN 003-6951((2010)

[50] L.Wipf: *Cryogenics*, **31**,936(1991)


UNIVERSITY
OF TROMSØ